

Tectonic evolution of NW Iberia during the Paleozoic inferred from the geochemical record of detrital rocks in the Cantabrian Zone

Daniel Pastor-Galán^{a,b,*}, Gabriel Gutiérrez-Alonso^b, Javier Fernández-Suárez^c,
Brendan Murphy^d, Fernando Nieto^e

^a Department of Earth Sciences, Paleomagnetic Laboratory "Fort Hoofddijk", Utrecht University, Budapestlaan 17, 3584 CD Utrecht, The Netherlands

^b Departamento de Geología, Universidad de Salamanca, Facultad de Ciencias, 37008 Salamanca, Spain

^c Departamento de Petrología y Geoquímica, Universidad Complutense and IGEO, CSIC, 28040 Madrid, Spain

^d Department of Earth Sciences, St. Francis Xavier University, Antigonish, Nova Scotia B2G 2W5, Canada

^e Departamento de Mineralogía y Petrología, Universidad de Granada, Avenida Fuentenueva s/n, 18002 Granada, Spain

ABSTRACT

The Cantabrian Zone of NW Iberia preserves a voluminous, almost continuous, sedimentary sequence that ranges in age from Ediacaran to Early Permian. Its tectonic setting is controversial and recent hypotheses include (i) passive margin deposition along the northern margin of Gondwana, (ii) an active continental margin, or (iii) the margin of a drifting ribbon continent and (iv) a combination of the three aforementioned possibilities. In this paper we present geochemical data from 21 samples taken in detrital rocks in the Cantabrian Zone from Ediacaran to Early Permian age. The results, together with previously published detrital zircon ages from these strata, allow a comprehensive analysis of changing tectonic scenarios and provenance through time. Collectively, these data indicate that this portion of Iberia was an active margin during the Ediacaran that evolved to become part of the passive margin of Gondwana at least from Ordovician to Late Devonian times. Changes in geochemistry, zircon age distribution and Sm/Nd isotopes during the Carboniferous are attributed to the far-field effects of the onset of the collision between Gondwana and Laurussia, and related processes such as recycling of older sedimentary sequences, as well as the involvement of the rocks formed during the Variscan orogeny and oroclinal buckling. Latest Carboniferous and Permian show a more juvenile Sm/Nd and higher values of illite crystallinity that may support the hypothesis of lithospheric foundering after oroclinal buckling.

Keywords: Cantabrian Zone; Paleozoic passive margin; Gondwana margin; Rheic Ocean; Orocline

1. Introduction

Knowledge on the tectonic evolution of sedimentary basins is fundamental to our overall understanding of geological processes operating throughout Earth history as well as for exploration of natural resources. In addition to the classical stratigraphy and sedimentology, the tectonic setting of sedimentary basins can be constrained by geochemical and isotopic analyses of detrital rocks (e.g. Bhatia, 1983; Murphy and Nance, 2002; Taylor and McLennan, 1985). The chemical composition of detrital rocks depends on numerous factors such as the composition of source areas, as well as the degree of weathering, diagenesis and metamorphism. For example REEs (rare earth elements) have low residence times in oceanic waters and typically preserve characteristics inherited from source regions. Although the use of tectonic discrimination diagrams (e.g. Bhatia, 1983; Bhatia and Crook, 1986; McLennan et al., 1993; Roser and Korsch, 1986) is controversial (e.g. Armstrong-Altrin

and Verma, 2005; Ryan and Williams, 2007), in general the geochemistry of sedimentary rocks, including discrimination and spider diagrams, provides insights into the evolution of basins in time and space, especially when combined with stratigraphy, geochronology, Sm/Nd isotopic systematics and X-ray diffraction (e.g. McLennan et al., 1993; Dostal and Keppie, 2009; Spalletti et al., 2012; Fuenlabrada et al., 2012).

The Cantabrian Zone of NW Iberia (Fig. 1) preserves an almost continuous stratigraphic sequence from Upper Ediacaran to Lower Permian (Fig. 2) that is thought to have been deposited on the northern Gondwanan margin (e.g. Nance et al., 2010; Pastor-Galán et al., 2013; Robardet, 2002, 2003). In this paper, we present new geochemical, Sm–Nd isotopic systematics and X-ray diffraction data from representative samples in this sequence as well as a compilation of previously published detrital zircon data to further constrain the tectonic evolution of NW Iberia and the evolution of the northern margin of Gondwana during the Paleozoic. The aims of our study are: (i) geochemical characterization of the detrital rocks of the Cantabrian Zone, (ii) to constrain their possible sources and (iii) to deduce tectonic settings as well as the exhumation and erosion of the different units involved in the Variscan orogenic event and subsequent oroclinal development.

* Corresponding author.

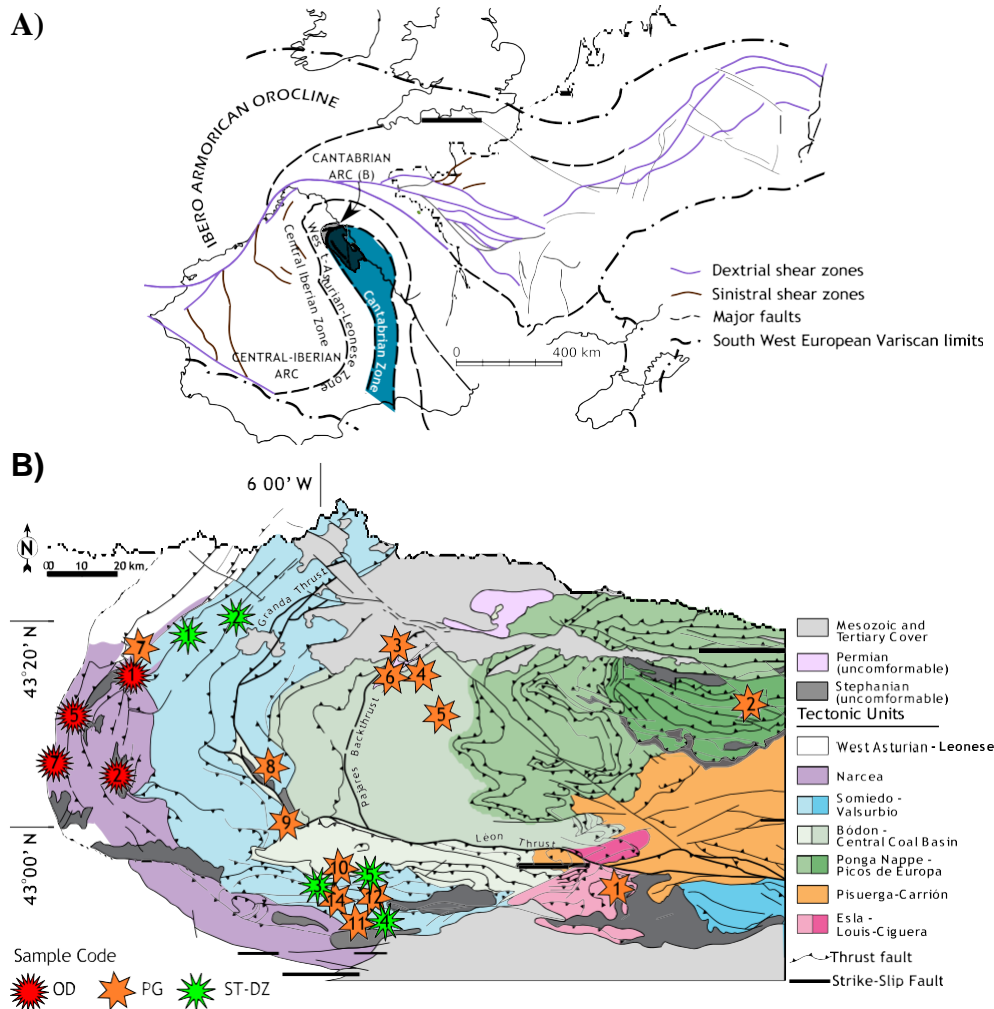


Fig. 1. A) Geographical situation of the Cantabrian Zone and adjacent tectonostratigraphic zones. B) Map of the Cantabrian zone. Stars represent the approximate location of the studied samples. For precise sample situation see Supplementary file 2 (.kml file).

2. Geological background

2.1. Tectonic history

In the Late Neoproterozoic and Early Cambrian, a long history of subduction and accretion of island arcs occurred along the northern margin of Gondwana (D'Lemos et al., 1990; Linnemann et al., 2007, 2008; Murphy and Nance, 1989; Murphy et al., 2000; Nance and Linnemann, 2008; Pereira et al., 2012). In Late Cambrian–Early Ordovician, a protracted period of rifting opened the Rheic Ocean with the separation of several peri-Gondwanan terranes from the northern margin of Gondwana (e.g. Montero et al., 2007; Murphy et al., 2006; Nance et al., 2010; Pereira et al., 2012; Sanchez-Garcia et al., 2008). The origin of this rifting episode is controversial; Murphy et al. (2006) suggested that slab pull due to ridge subduction underneath Laurentia would result in rifting along the Gondwanan margin and eventually the formation of the Rheic Ocean. In contrast, other authors (e.g. Díez Fernández et al., 2012; Martínez Catalán et al., 2009) maintain that subduction roll-back initiated the opening of Rheic Ocean. This period of rifting and early drift is recorded in NW Iberia by widespread rift-related igneous activity with ages between 495 and 470 Ma (Bea et al., 2006; Díez Montes, 2006; Gutiérrez-Alonso et al., 2007; Heinz et al., 1985; Montero et al., 2009; Murphy et al., 2008; Rubio-Ordóñez et al., 2012; Sánchez-García et al., 2003, 2008; Valverde-Vaquero and Dunning, 2000; Valverde-Vaquero et al., 2006) and by the coeval accumulation

of a thick passive margin sequence (e.g. Aramburu et al., 2002). The Rheic Ocean is interpreted to have reached its greatest width (ca. 4000 km) during the Silurian (Nance et al., 2010 and references therein). One of the main disputations in the evolution of Rheic Ocean is the paleoposition of NW Iberia, Armorica and other terranes involved in the Variscan orogeny during Silurian and Devonian times. On the basis of paleomagnetic data, some authors interpret NW Iberia during the Late Silurian to be part of a drifting ribbon continent variously called Armorica, the Hun terrane or the Galatia terrane (e.g. Stampfli and Borel, 2002; Stampfli et al., 2013; Tait, 1999; Tait et al., 1994; Torsvik and Cocks, 2004; Torsvik et al., 2012; Van Der Voo, 1982, 1988; van der Voo, 1993). In this scenario, the drifting of Armorica from Gondwana is responsible for the opening of the Paleotethys Ocean and its collision against Laurentia for the closure of the Rheic Ocean and the onset of Variscan orogenesis. Usually those models imply subduction towards both Rheic margins, northern Gondwana and southern Laurussia (e.g. Stampfli and Borel, 2002) or synchronous subduction along both sides of the Armorican terrane including a southward subduction of Rheic and a northward subduction of Paleotethyan oceanic lithospheres (Stampfli et al., in press). Other authors, however, place Iberia along the northern Gondwana passive margin throughout the Paleozoic (Barreiro et al., 2006; Díez Fernández et al., 2010; Fernandez-Suarez et al., 2006; Gutiérrez-Alonso et al., 2008; Linnemann et al., 2004, 2008; López-Guijarro et al., 2008; Martínez Catalán et al., 2007, 2009; Murphy et al., 2006; Pastor-Galán et al., 2013; Quesada, 1991, 2006;

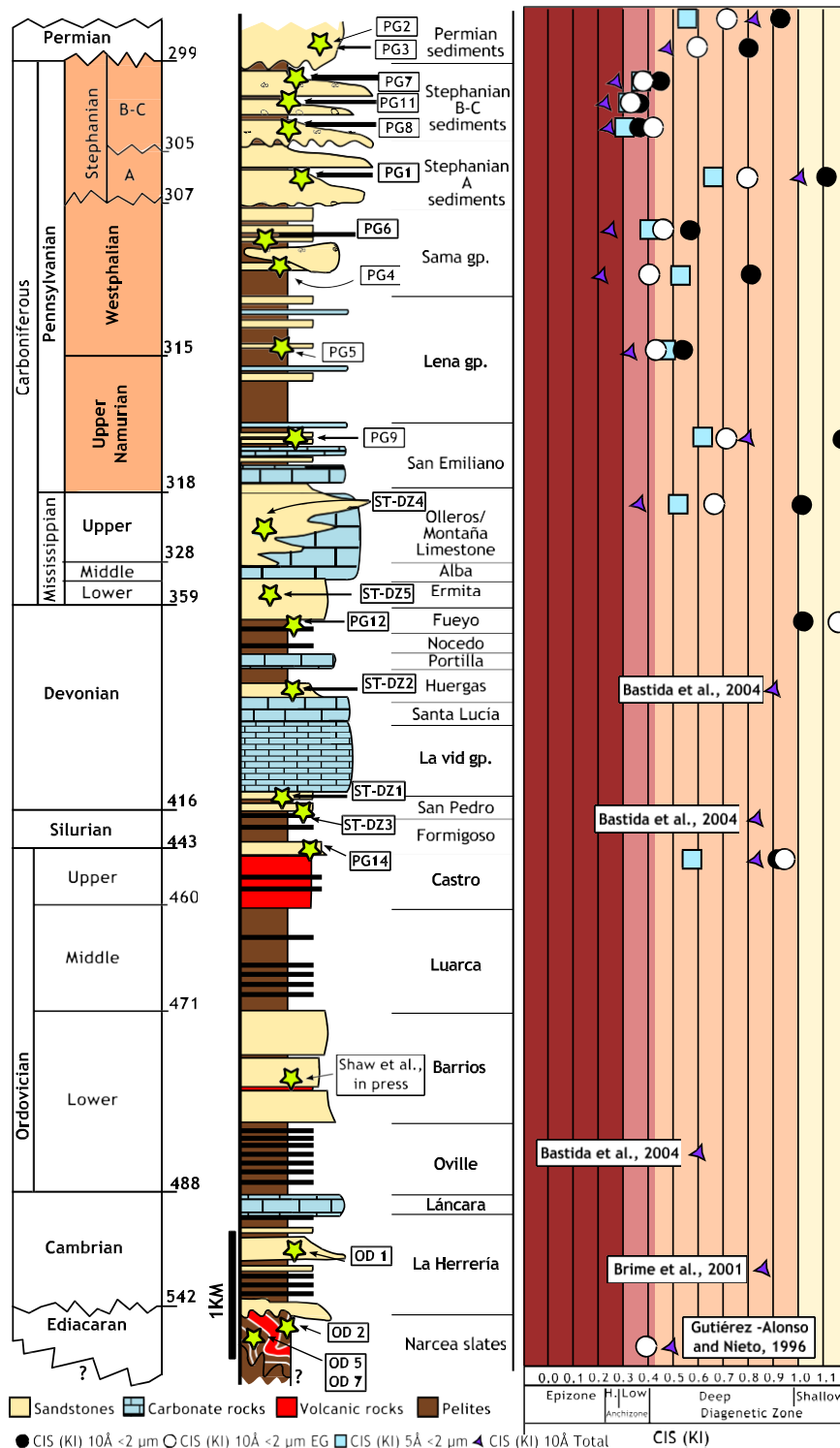


Fig. 2. Synthetic stratigraphic column for the Cantabrian Zone (modified from Pastor-Galán et al., 2013 and after Bastida, 2004) with the location of the studied samples and the samples used from the literature. In the right side, there is a graph summarizing the results of XRD (crystallinity) analyses.

Robardet, 2002, 2003), and most of these models consider that subduction of Rheic Ocean lithosphere, which began in the Early Devonian, was directed northward i.e. away from the Gondwanan margin.

In both scenarios, the closure of the Rheic Ocean is recorded by the deformation associated with the final collision between Laurussia and Gondwana or Armorica and in some ophiolitic suites preserved in the suture zone between these continents (e.g. Arenas et al., 2007a,b). Continental collision began at ca. 365 Ma (Dallmeyer et al., 1997) and

continued shortening eventually led to the extensional collapse of the thickened hinterland at ca. 320 Ma (Arenas and Martínez Catalán, 2003; Martínez Catalán et al., 2009). The latter event is coeval with the initial development of the non-metamorphic foreland fold-thrust belt along the Gondwanan margin (e.g. Pérez-Estaún et al., 1994), which is exposed only in the Cantabrian Zone of NW Iberia.

The tectonostratigraphic zonation of Variscan orogen in Iberia shows an "S" shape pattern recently interpreted as a double orocline consisting

of a northern and southern arc (Martínez Catalán, 2011; Martínez Catalán, 2012; Shaw et al., 2012; Weil et al., 2013; Fig. 1). Although the formation of both orogen-scale arcs might be related (Martínez Catalán, 2011; Pastor-Galán, 2013; Shaw et al., 2012), only the kinematics of the northern arc has been resolved. The northern arc, known as Cantabria–Asturias Arc (e.g. Weil et al., 2001) or Cantabrian Orocline (e.g. Gutiérrez-Alonso et al., 2012; Weil et al., 2013), was developed after closure of the Rheic Ocean and the building and collapse of the Variscan orogenic edifice and, therefore, is considered post-Variscan in age (Pastor-Galán et al., 2011; Weil et al., 2001). Gutiérrez-Alonso et al. (2004) proposed a thick-skinned model for this oroclinal development which involves lithospheric-scale rotation of the orogen limbs, with extension in the outer arc resulting in thinning of the mantle lithosphere, and coeval shortening in the uppermost crust (Alvarez-Marrón and Perez-Estaún, 1988; Julivert and Arboleya, 1986; Julivert and Marcos, 1973) and lithospheric thickening in the inner arc (Gutiérrez-Alonso et al., 2004, 2010; Pastor-Galán et al., 2012a,b). The latter process resulted in gravitational instability causing foundering and removal of the mantle lithosphere from the lower crust that was followed by asthenospheric upwelling and high heat flow which triggered voluminous Late Carboniferous–Permian magmatism in the Variscan fold-and-thrust belt (Fernandez-Suarez et al., 2000; Fernández-Suárez et al., 2011; Gutiérrez-Alonso et al., 2004, 2011a,b; Pastor-Galán et al., 2012c,d).

2.2. The Cantabrian Zone and its stratigraphy

The Cantabrian Zone is situated in the core of the Cantabrian Orocline (Gutiérrez-Alonso et al., 2004; Pérez-Estaún et al., 1988; Weil, 2006) (Fig. 1A and B) and is a classical foreland fold-and-thrust belt characterized by thin-skinned tectonics with a transport direction towards the core of the arc (Merino-Tomé et al., 2009; Pérez-Estaún et al., 1988). This zone of the orogen is characterized by locally developed non-penetrative cleavage and low finite strain values (Gutiérrez-Alonso, 1996; Pastor-Galán et al., 2009). Illite crystallinity and conodont color alteration indexes indicate non-metamorphic to very low-grade metamorphic conditions (Bastida et al., 2004; Brime et al., 2001; García-López et al., 2007; Gutiérrez-Alonso and Nieto, 1996). The first record of tectonic instability, due to the loading in the hinterland, is interpreted to have occurred in the upper Devonian (García-Ramos, 1978; García Ramos and Colmenero, 1981; Keller et al., 2008; Rodríguez-Fernández, 1991) but the sedimentary record of a fore-bulge and a fore-deep is not evident

until the Lower Carboniferous (Colmenero et al., 1993, 2002). Deformation began in the earliest Pennsylvanian (Dallmeyer et al., 1997, ca. 321Ma.) and resulted in the development of several clastic wedges related to the emplacement of different thrust units (Marcos and Pulgar, 1982).

The Cantabrian Zone stratigraphic column is almost complete from Ediacaran to Lower Permian. However, four unconformities have been documented (Fig. 2) and are interpreted to reflect the different tectonic pulses described above (e.g. Alonso, 1989; Gutiérrez-Alonso, 1996; Pastor-Galán et al., 2011).

The overall stratigraphy is given in Table 1 and a detailed description of each formation is given in Bastida (2004) and references therein. The stratigraphic succession starts with a thick Ediacaran sequence that crops out in the Narcea Antiform in the western and southern areas of the Cantabrian Zone. The whole Ediacaran sequence has been known classically as the Narcea Slates (Lotze, 1945). Although its thickness is undetermined, this Ediacaran succession is interpreted as a thick conformable sequence of turbiditic strata (Gutiérrez-Alonso, 1996). Rubio Ordóñez (2010) divided this sequence in two different stratigraphic units, according to their relative age (Fernández-Suárez et al., 1998; Gutiérrez-Alonso et al., 2004), and nature of the volcanic clasts (Rubio-Ordóñez et al., in press). This division is also supported by the detrital zircon content of both sequences (Fernández-Suárez et al., in press).

The Ediacaran sequence is unconformably overlain by pre-Variscan Paleozoic clastic and carbonate platformal strata (Fig. 2) that vary in thickness from 6500 m in the west to about 1000 m in the east (Marcos and Pulgar, 1982) and includes a Lower Cambrian succession of 1000–1500 m of feldspathic sandstone, quartzite, shale and conglomerate layers followed by Middle Cambrian limestones (ca. 200 m) and Late Cambrian shales and sandstones (from west to east 1600 to 200 m) that evolve to quartzites at Early Ordovician (1000 to 80 m from west to east). Middle and Late Ordovician correspond with a thin and sometimes absent alternating black shales with some volcanics. Following its distinctive sequence of Silurian black shale and iron-rich sandstone with a thickness between 450 m and 75 m (from west to east; Fig. 2). The pre-Variscan strata culminate with a Devonian and Early Carboniferous (Mississippian) succession consisting of alternating carbonate and siliciclastic strata (Fig. 2) in which several transgressions and regressions have been documented (Aramburu et al., 2002; Gibbons and Moreno, 2002; Hofmann and Keller, 2006; Keller et al., 2008). Paleocurrent data recorded in the pre-Variscan strata indicate

Table 1
Synthesis of the sampled rocks.

| Sample no. | Formation | Aprox. depositional age | Characteristics |
|------------|----------------|-------------------------|---|
| OD5 | Narcea slates | 600 | Turbidites with interbedded volcanics |
| OD7 | Narcea slates | 600 | Turbidites with interbedded volcanics |
| OD2 | Narcea slates | 545 | Turbidites with interbedded volcanics |
| OD1 | Herrería | 535 | Alternating shales, feldspathic sandstone and micro-conglomerates |
| Literature | Barrios | 477 | Quartzite |
| PG14 | Formigoso | 430 | Black shale |
| ST-DZ3 | San Pedro | 419 | Ironstones with interbedded shales |
| ST-DZ1 | San Pedro | 410 | Ironstones with interbedded shales |
| ST-DZ2 | Huergas | 395 | Shales and sandstones |
| PG12 | Fueyo | 374 | Shales with small sand layers |
| ST-DZ5 | Ermita | 370 | Quartzite siltstone |
| ST-DZ4 | Olleros | 320 | Turbidite |
| PG9 | San Emiliano | 318 | Intercalated limestones and sandstones |
| PG5 | Lena Group | 315 | Siliciclastics with minor carbonate layers |
| PG4 | Sama Group | 313 | Sandstones, conglomerates and shales with coal seams |
| PG6 | Sama Group | 311 | Sandstones, conglomerates and shales with coal seams |
| PG1 | Stephanian A | 307 | Sandstones, conglomerates and shales with coal seams |
| PG11 | Stephanian B–C | 305 | Sandstones, conglomerates and shales with coal seams |
| PG8 | Stephanian B–C | 304 | Sandstones, conglomerates and shales with coal seams |
| PG7 | Stephanian B–C | 303 | Sandstones, conglomerates and shales with coal seams |
| PG3 | Sotres | 295 | Red Sandstones with volcanics |
| PG2 | Sotres | 292 | Red Sandstones with volcanics |

that their sediment source was located to the east in present-day coordinates (Fernández-Suárez et al., 1998; Shaw et al., 2012) but there are no currently exposed potential source rocks.

The pre-Variscan succession is overlain conformably by an up to 5000 m thick Westphalian A (Bashkirian–Moskovich) syn-orogenic sequence dominated by shallow marine and interbedded continental clastic strata. This sequence is in turn unconformably overlain by Stephanian (Upper Pennsylvanian) and Permian rocks, mostly of continental nature (Figs. 1 and 2).

The Stephanian strata are characterized by coal-bearing continental clastic rocks including conglomerates, sandstones and mudstones (e.g. Colmenero et al., 2008; Fig. 2). This succession shows similar stratigraphic and sedimentological characteristics over much of northern Iberia implying that it overlies much of the western and southern portions of the Cantabrian Zone and the adjacent West Asturian–Leonese Zone (Corrales, 1971; Pastor-Galán et al., 2011). Stephanian rocks crop out in synclines, are not internally deformed and their overall structural characteristics suggest that deposition occurred after the bulk of Variscan deformation had taken place (Pastor-Galán et al., 2011, 2012b).

In contrast to the regionally deposited Stephanian strata, Permian strata were deposited in localized basins (Martínez-García, 1991; Suárez, 1988) that post-date the formation of the Cantabrian Orocline (Pastor-Galán et al., 2011; Weil et al., 2010). These strata are only moderately tilted and are not internally deformed. The dominant lithologies are continental red conglomerates, red shales and sandstones, with minor limestones, volcanoclastic rocks, calc-alkaline basaltic lava flows and scarce coal seams (Martínez-García, 1981; Suárez, 1988).

2.3. Sampling strategy

We selected 21 samples of detrital rocks whose depositional age ranges from 600 to 292 Ma, representing the entire Ediacaran to Late Paleozoic stratigraphic succession (Figs. 1, 2). We present a synthesis of the stratigraphy, sedimentological characteristics and depositional age of the sampled rocks in Table 1. In general we selected at least one sample from each of the most representative and known formations as described in Bastida (2004). Additionally, we also collected samples within the same formation in order to obtain a better resolution of the significance of different events marked by unconformities. For example, we sampled the Ediacaran series in three different localities (OD5 and OD7, lower unit; OD2, upper unit). We also obtained two samples of Upper Silurian to Lower Devonian ironstone of the San Pedro Fm, an ironstone with interbedded shales (ST-DZ3 and ST-DZ1 respectively) due to its special iron rich composition. These strata are typical of similarly-aged ironstones found elsewhere in the Variscan belt (e.g. Guerrak 1987a,b; Gloaguen et al., 2007) and were deposited in a shallow shelf setting (Suárez de Centi, 1988) close to the transition from non-marine to marine environments (Van Houten, 1985; Young, 1989).

In addition, we sampled thoroughly the Upper Paleozoic stratigraphic succession to better track the effects of Variscan and post-Variscan tectonic processes on the geochemical and isotopic composition of the sedimentary rocks. Specifically, we sampled Stephanian sandstones in four different locations and different stratigraphic positions (PG1, Stephanian A; PG11; PG8 and PG7, from older to younger, Stephanian B–C) as well as Permian undeformed sandstones (PG2 and PG3) of roughly the same depositional age in two different locations (Figs. 1 and 2).

Finally, we include the major and trace element data from Shaw et al. (in press) of the Early Ordovician Barrios Fm (Table 1) (Gutiérrez-Alonso et al., 2007) which is the correlative of the regionally-deposited Armorican Quartzite in the study area (e.g. Aramburu et al., 2002; Gutiérrez-Marco et al., 1999, 2002). However no isotopic data are available from this formation.

3. Analytical methods and results

All 21 samples were analyzed for major, trace and rare earth elements (REEs) and for Sm–Nd isotopes. Major and selected trace elements (Rb, Sr, Ba, Zr, Nb, Y, Zn, V, Cr and Ni) were analyzed by X-ray fluorescence using a Philips PW2400 for at the Nova Scotia Regional Geochemical Centre at Saint Mary's University, Canada. Details of analytical methods as well as precision and accuracy of the X-ray data are reported by Dostal et al. (1994). The analytical procedure for REE and other trace elements was as follows: (i) sintering of a 0.2 g sample aliquot with sodium peroxide, (ii) dissolution of the sinter cake and separation and dissolution of REE hydroxide-bearing precipitate, and

(iii) analysis by ICP-MS using the method of internal standardization to correct for matrix and drift effects were performed at the Memorial University of Newfoundland. Details of these procedures can be found in Longrich et al. (1990).

Sm–Nd isotopic analyses were performed at the Atlantic Universities Regional Isotopic Facility at Memorial University on a Finnigan MAT 262V TIMS mass spectrometer in static mode. Further information on analytical procedures is given in Kerr et al. (1995). Nd isotopic ratios are normalized to $^{146}\text{Nd}/^{144}\text{Nd} = 0.7219$. The reported values were adjusted to La Jolla Nd standard ($^{143}\text{Nd}/^{144}\text{Nd} = 0.511860$). During the course of data acquisition, replicates of the standard gave a mean value of $^{143}\text{Nd}/^{144}\text{Nd} = 0.511888 \pm 16$ (2σ , $n = 12$). The in-run precision on Nd isotopic ratios is given at 95% confidence level. Errors on Nd isotopic compositions are $\pm 0.002\%$ and errors on the $^{147}\text{Sm}/^{144}\text{Nd}$ ratio are estimated to be less than 0.1%.

We analyzed the samples labeled PG by X-ray diffraction (XRD, see Fig. 2 and Table 1). Those samples correspond to strata for which no XRD data were available in the literature (García-López et al., 2007, 2013). The fourteen studied samples were washed and, after coarse crushing, homogeneous rock chips were used for preparation of X-ray diffraction (XRD) samples to determine the overall trends in mineral assemblages and record any variations in metamorphic grade along the studied cross sections using the Kubler Index (Kubler, 1968). Currently, the Kubler Index is the most common method used to determine the metamorphic grade and to identify variations in the anchizone conditions between diagenesis and low-grade metamorphism in metapelitic sequences. This index is based in the measurement of the full peak width at half maximum intensity of the first, 10 Å , X-ray powder diffraction peak of K-white mica and it is expressed as $\Delta 2\theta$ in the Bragg angle. Samples were analyzed using a PANalytical X'Pert Pro powder diffractometer equipped with a X'Celerator detector, CuK α radiation, operated at 45 kV and 40 mA, Ni filter and 0.25° divergence slit at the Departamento de Mineralogía y Petrología of the Universidad de Granada to study whole-rock samples and clay fractions ($> 2\text{ }\mu\text{m}$). The $< 2\text{-}\mu\text{m}$ fractions were separated by repeated extraction of supernatant liquid subsequent to centrifugation, following the Stokes' law. Oriented aggregates were prepared by sedimentation on glass slides. Ethylene glycol (EGC) treatment was carried out on the samples to corroborate the identification of illite–smectite or chlorite–smectite on the basis of the expansibility of these phases. Kubler Index was measured using a step increment of $0.008^\circ 2\theta$ and a counting time of 50 s/step. Our KI measurements (x) were transformed into crystallinity index standard (CIS) values (y) according to the equation $y = 1.8718x - 0.0599$. For a full description of the procedures see Abad et al. (2010).

4. Results

4.1. Whole rock geochemistry

Samples show a large variation in chemical composition with SiO_2 ranging from ca. 45% to 98% (on a volatile free basis, Table 2). Al, Mg, K, Ti and Fe display negative correlations with Si representing the varying proportions of clay/mud minerals and quartz-rich minerals, as it is common in siliciclastic rocks (Fig. 3; Bhatia, 1983; Li et al., 2005;

Table 2
Chemical composition of the studied rocks.

| | PG-1 | PG-2 | PG-3 | PG-4 | PG-5 | PG-6 | PG-7 | PG-8 | PG-9 | PG-11 | PG-12 | PG-14 | OD-1 | OD-2 | OD-4 | OD-7 | ST-DZ-1 | ST-DZ-2 | ST-DZ-3 | ST-DZ-4 | ST-DZ-5 |
|--------------------------------|-------|-------|--------|--------|-------|--------|--------|-------|--------|-------|-------|-------|--------|--------|-------|-------|---------|---------|---------|---------|---------|
| SiO ₂ | 87.54 | 72.09 | 82.64 | 79.75 | 81.75 | 79.26 | 76.13 | 75.29 | 60.05 | 78.32 | 90.51 | 90.88 | 87.01 | 69.4 | 78.43 | 66.94 | 80.65 | 92.04 | 46.78 | 89.54 | 98.2 |
| TiO ₂ | 0.401 | 0.474 | 0.48 | 0.566 | 0.471 | 0.828 | 0.652 | 0.654 | 0.636 | 0.618 | 0.268 | 0.428 | 0.272 | 0.759 | 0.6 | 0.953 | 0.337 | 0.227 | 0.268 | 0.279 | 0.171 |
| Al ₂ O ₃ | 5.55 | 8.63 | 7.81 | 10.42 | 8.4 | 12.43 | 12.42 | 11.77 | 11.77 | 9.75 | 2.87 | 3.86 | 5.99 | 14.61 | 9.87 | 14.91 | 2.1 | 2.05 | 2.85 | 3.1 | 0.69 |
| Fe ₂ O ₃ | 2.36 | 2.55 | 1.3 | 3.7 | 3.02 | 0.66 | 3.49 | 4.75 | 3.97 | 3.84 | 3.25 | 1.83 | 1.86 | 4.99 | 3.57 | 5.44 | 14.43 | 4.14 | 44.83 | 1.79 | 0.48 |
| MnO | 0.03 | 0.065 | 0.04 | 0.018 | 0.017 | 0 | 0.022 | 0.028 | 0.048 | 0.046 | 0.011 | 0.006 | 0.004 | 0.054 | 0.017 | 0.03 | 0.033 | 0.017 | 0.246 | 0.056 | 0.017 |
| MgO | 0.05 | 0.46 | 0.45 | 0.15 | 0.54 | 0.23 | 0.96 | 0.94 | 1.19 | 0.88 | 0.02 | 0.17 | 0.37 | 1.57 | 1.14 | 2.6 | 0.36 | 0.2 | 0.48 | 0.41 | 0.06 |
| CaO | 0.37 | 6.05 | 1.61 | 0.03 | 0.14 | 0.02 | 0.16 | 0.1 | 9.33 | 0.23 | 0.02 | 0.02 | 0.05 | 0.36 | 0.03 | 0.33 | 0.51 | 0.07 | 0.94 | 1.66 | 0.02 |
| Na ₂ O | 0 | 0 | 0.87 | 0.05 | 0.71 | 0.08 | 0.69 | 0.06 | 0.08 | 1.01 | 0.1 | 0 | 0 | 3.58 | 0.76 | 3.73 | 0.01 | 0 | 0.1 | 0.26 | 0 |
| K ₂ O | 0.83 | 2.32 | 1.36 | 1.67 | 1.48 | 2.14 | 2.33 | 2.51 | 1.64 | 1.71 | 0.53 | 0.78 | 3.39 | 2.1 | 1.66 | 1.45 | 0.3 | 0.46 | 0.29 | 0.56 | 0.15 |
| P ₂ O ₅ | 0.096 | 0.118 | 0.106 | 0.093 | 0.118 | 0.068 | 0.117 | 0.109 | 0.139 | 0.138 | 0.05 | 0.063 | 0.053 | 0.183 | 0.11 | 0.226 | 0.45 | 0.03 | 0.914 | 0.065 | 0.029 |
| LOI | 2.31 | 6.90 | 3.57 | 3.60 | 2.78 | 4.12 | 3.26 | 3.50 | 11.43 | 2.68 | 1.75 | 1.28 | 1.15 | 2.45 | 2.96 | 2.83 | 0.83 | 0.79 | 2.31 | 2.27 | 0.20 |
| Sum | 99.54 | 99.66 | 100.24 | 100.05 | 99.43 | 99.84 | 100.23 | 99.71 | 100.28 | 99.22 | 99.38 | 99.32 | 100.15 | 100.06 | 99.15 | 99.44 | 100.01 | 100.02 | 100.01 | 99.99 | 100.02 |
| V | 45 | 52.5 | 44 | 80.5 | 65.4 | 94 | 103.7 | 103.3 | 122.9 | 68.4 | 19.9 | 21.7 | 33.4 | 97.9 | 76.2 | 123.3 | 81 | 76 | 202.9 | 35.8 | 13.3 |
| Cr | 205.6 | 154 | 153.5 | 136.9 | 169.3 | 159.7 | 227.8 | 175.7 | 110.2 | 192.3 | 288.4 | -9.2 | 2.7 | 72.2 | 57.6 | 106 | 222.8 | 282.1 | 113.6 | 213.4 | 282.4 |
| Co | 11.6 | 10.7 | 8.3 | 8.8 | 10 | 3 | 11.9 | 6.9 | 13.8 | 11.5 | 7.5 | 122.1 | 142.5 | 43.1 | 38.3 | 27.4 | 5.1 | 9.3 | 26.5 | 6 | 1.5 |
| Ni | 21 | 26.6 | 16.5 | 16.6 | 23.4 | 6.7 | 37.6 | 24.7 | 40 | 28.1 | 12.6 | 11.3 | 11.7 | 32.3 | 12.6 | 34.9 | 11.8 | 21.7 | 27.8 | 13.2 | 7.8 |
| Cu | 5.3 | 75.8 | 9.9 | 8.1 | 5.7 | 8 | 24.5 | 17.7 | 13.2 | 14.7 | 5.2 | 3.8 | 0.6 | 22.6 | 13.5 | 16.4 | 5 | 5.1 | 9.7 | 6.6 | 2.7 |
| Zn | 57.9 | 12 | 23.1 | 19.5 | 47.3 | 8.2 | 80.9 | 34.8 | 83.9 | 59.4 | 51.6 | 18.7 | 20.4 | 47.9 | 51.4 | 37.3 | 15 | 22.3 | 12.2 | 11 | 5.3 |
| Ga | 7.2 | 10.3 | 8.7 | 13.6 | 10.5 | 16.1 | 15.5 | 15.4 | 16.6 | 12.4 | 3.7 | 3.7 | 5.8 | 17.4 | 13.7 | 19.1 | 2.5 | 1.4 | 6 | 1.7 | 0.1 |
| Rb | 31 | 75.2 | 50.5 | 71.7 | 62.3 | 87.5 | 95.2 | 100.3 | 75.7 | 66.5 | 15.4 | 25.9 | 72.8 | 78.3 | 60.2 | 52.1 | 14.1 | 38.8 | 18.5 | 21.5 | 5.3 |
| Sr | 98.8 | 89.2 | 82.7 | 54.1 | 62.5 | 134.8 | 62.9 | 55.8 | 191.5 | 78 | 21.9 | 15.5 | 26.8 | 178.8 | 33.1 | 179.4 | 27.9 | 24.2 | 87.5 | 62.4 | 12.6 |
| Y | 16.4 | 26.5 | 24.1 | 23.7 | 19.3 | 28 | 27.7 | 22.2 | 33.4 | 23.6 | 17.6 | 27.5 | 17.3 | 28.2 | 20.3 | 36.7 | 40.4 | 15.6 | 70.5 | 11.4 | 6.4 |
| Zr | 203.8 | 271.6 | 350.1 | 137.4 | 159.9 | 487.4 | 173.3 | 179.8 | 291.6 | 188.7 | 196.1 | 230 | 104 | 213.6 | 215.7 | 282.7 | 213.9 | 150.1 | 99.3 | 239.2 | 392 |
| Nb | 9.3 | 10.6 | 11.4 | 13.2 | 10.4 | 16.4 | 13.4 | 13.5 | 16 | 11 | 5.6 | 9.4 | 10.5 | 13 | 10.2 | 15.8 | 7.4 | 3.2 | 10 | 1.1 | 0 |
| Ba | 85.8 | 168.8 | 203.3 | 304.3 | 230.4 | 407.9 | 512.5 | 434.3 | 219.2 | 324.1 | 141.3 | 119.3 | 361.9 | 450.5 | 419 | 380.7 | 50 | 51.8 | 144.8 | 75.2 | 9.1 |
| La | 29 | 38.9 | 36 | 36.4 | 34 | 48.5 | 35.8 | 41.2 | 49.2 | 38.7 | 23 | 25 | 32.3 | 30.6 | 32.2 | 38 | 29.8 | 22.5 | 51.6 | 12.2 | 12.3 |
| Pb | 13.6 | 6.8 | 11.6 | 23.9 | 12.9 | 15.2 | 18.3 | 7.9 | 19.2 | 14.6 | 12.2 | 12.8 | 9.5 | 9.9 | 17.6 | 7.3 | 11.1 | 7.9 | 1.6 | 10.5 | 10 |
| Th | 11.8 | 14.1 | 11 | 11.7 | 10.2 | 16.9 | 13.6 | 13 | 13.7 | 10.3 | 9.6 | 11.2 | 11 | 10.7 | 11.8 | 14.5 | 13.7 | 12.8 | 13.3 | 7.4 | 7.9 |
| U | 2.2 | 2.9 | 4.5 | 2.1 | 6.1 | 5.2 | 2.3 | 5.2 | 2.3 | 3.8 | 3.9 | 3.2 | 4.2 | 4.7 | 4.3 | 3.9 | 0.8 | 0 | 4.1 | 5.2 | 2.7 |
| Ce | 58.8 | 71.2 | 67.7 | 61.4 | 67.5 | 86.6 | 76.7 | 70.9 | 77.1 | 71.2 | 50.2 | 58.8 | 74.5 | 62.3 | 73.4 | 72 | 45.7 | 41.1 | 79.6 | 25.1 | 14.9 |
| Nd | 21.6 | 27.5 | 28.3 | 23.9 | 22 | 48.5 | 35.7 | 31.6 | 41.2 | 28.8 | 17.4 | 18 | 19.6 | 28.7 | 27.6 | 37.6 | 25.3 | 13.1 | 40.1 | 9.7 | 9.1 |
| Cs | 5.8 | 7.4 | 6.6 | 3.7 | 5.7 | 9.3 | -0.2 | 5.7 | 5.6 | 4.2 | 3.4 | 1.6 | 2.6 | 1.4 | 3.1 | 0.3 | 2 | 14.9 | 0 | 6.5 | 5.2 |
| Pr | 3.898 | 6.371 | 5.824 | 5.503 | 5.468 | 10.011 | 8.085 | 7.201 | 7.642 | 7.364 | 2.588 | 3.813 | 3.599 | 6.848 | 6.077 | 8.602 | 5.632 | 3.135 | 9.149 | 2.813 | 1.096 |
| Sm | 2.930 | 4.476 | 4.413 | 3.404 | 3.989 | 6.859 | 5.848 | 5.040 | 5.721 | 5.769 | 2.302 | 3.412 | 2.284 | 5.313 | 4.271 | 6.830 | 5.796 | 2.076 | 8.976 | 2.332 | 0.737 |
| Eu | 0.633 | 0.892 | 0.768 | 0.674 | 0.777 | 1.205 | 1.196 | 0.979 | 1.196 | 1.131 | 0.532 | 0.836 | 0.526 | 1.231 | 0.978 | 1.426 | 1.613 | 0.383 | 2.228 | 0.425 | 0.105 |
| Gd | 2.652 | 4.020 | 3.563 | 2.868 | 3.176 | 4.910 | 4.750 | 3.987 | 4.987 | 4.617 | 2.564 | 3.486 | 2.487 | 4.324 | 3.386 | 6.292 | 6.179 | 2.151 | 10.004 | 2.187 | 0.689 |
| Tb | 0.379 | 0.536 | 0.526 | 0.433 | 0.444 | 0.712 | 0.720 | 0.584 | 0.772 | 0.675 | 0.407 | 0.621 | 0.371 | 0.691 | 0.520 | 0.896 | 0.971 | 0.312 | 1.537 | 0.329 | 0.115 |
| Dy | 2.213 | 3.209 | 2.882 | 2.693 | 2.652 | 4.441 | 4.100 | 3.699 | 4.477 | 3.503 | 2.220 | 3.799 | 2.142 | 4.095 | 2.908 | 5.498 | 5.882 | 2.133 | 10.809 | 1.983 | 0.717 |
| Ho | 0.468 | 0.688 | 0.636 | 0.602 | 0.489 | 0.882 | 0.783 | 0.714 | 0.877 | 0.696 | 0.423 | 0.734 | 0.381 | 0.804 | 0.565 | 1.057 | 1.196 | 0.453 | 2.260 | 0.408 | 0.174 |
| Er | 1.306 | 1.948 | 1.904 | 1.674 | 1.447 | 2.596 | 2.265 | 2.052 | 2.474 | 2.008 | 1.116 | 2.030 | 1.053 | 2.323 | 1.652 | 3.121 | 3.627 | 1.483 | 6.911 | 1.279 | 0.584 |
| Tm | 0.190 | 0.288 | 0.270 | 0.264 | 0.210 | 0.416 | 0.311 | 0.306 | 0.363 | 0.290 | 0.146 | 0.286 | 0.157 | 0.345 | 0.245 | 0.456 | 0.458 | 0.213 | 1.123 | 0.197 | 0.079 |
| Yb | 1.313 | 2.020 | 1.858 | 1.588 | 1.387 | 2.709 | 2.165 | 1.984 | 2.326 | 1.845 | 1.042 | 1.871 | 0.976 | 2.298 | 1.848 | 2.966 | 3.051 | 1.389 | 7.423 | 1.349 | 0.739 |
| Lu | 0.190 | 0.301 | 0.281 | 0.238 | 0.198 | 0.427 | 0.313 | 0.303 | 0.339 | 0.282 | 0.154 | 0.262 | 0.158 | 0.349 | 0.303 | 0.431 | 0.462 | 0.211 | 1.153 | 0.214 | 0.109 |
| Hf | 4.214 | 7.234 | 7.988 | 2.666 | 3.683 | 12.854 | 4.357 | 4.192 | 7.121 | 4.323 | 4.031 | 4.183 | 2.356 | 4.304 | 5.144 | 6.579 | 4.474 | 2.136 | 2.561 | 7.217 | 5.518 |
| Ta | 0.332 | 0.459 | 0.531 | 0.458 | 0.423 | 0.665 | 0.576 | 0.588 | 0.604 | 0.482 | 0.208 | 0.675 | 0.916 | 0.621 | 0.519 | 0.669 | 0.202 | 0.157 | 0.219 | 0.167 | 0.042 |

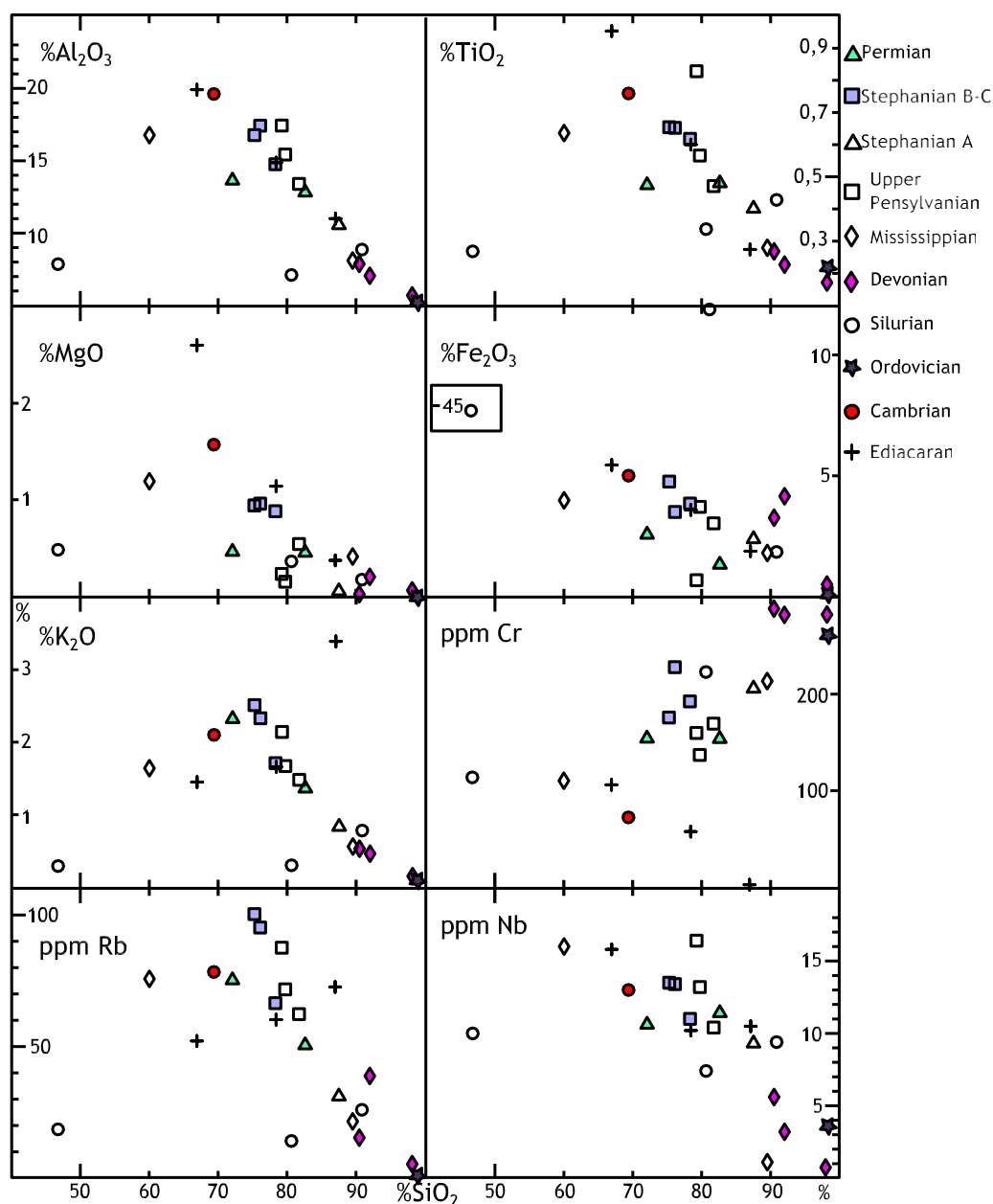


Fig. 3. Variation diagrams of SiO_2 vs. Al_2O_3 , TiO_2 , Fe_2O_3 , MgO , K_2O (wt.%), Rb, Nb and Cr (ppm). See text for explanation and discussion.

Dostal and Keppie, 2009; Spalletti et al., 2012) indicating that the lower values of SiO_2 correspond with poorly sorted or fine grained samples. The San Pedro Formation ironstone samples provide the only exception, but the relationship between FeO and SiO_2 is anomalous when compared with that of “normal” siliciclastic rocks (e.g. Bhatia, 1983).

The strong correlation between TiO_2 and Al_2O_3 (Fig. 4) suggests that Ti may be present predominantly in phyllosilicates (Li et al., 2005), however, Rb, La and Nb show positive correlation with Al and negative correlation with SiO_2 , which indicates that dilution of elements that do not partition into quartz could be applicable to TiO_2 as well. Contrariwise, Cr shows a positive correlation with SiO_2 although the pattern is less clear. In general, Cr in sedimentary clastic rocks is expected to reside mainly in clays or in secondary oxides (e.g. Meinhold et al., 2007). Given the negative correlation with Al_2O_3 , we infer that Cr is not primarily linked with the clay-mica fraction. Zr is scattered in both plots and shows positive correlations with Hf, Nb and REE, which implies that

this element is principally tied in accessory mineral phases, presumably zircon (see Table 2 and Supplementary file 1).

Most samples display moderately fractionated REE patterns (Fig. 5: Table 2), where LREE are enriched relative to HREE, which present a slightly depleted pattern with the exception of sample ST-DZ3 that shows a flat pattern and ST-DZ4 whose content in HREE is significantly lower than the rest of the samples. All samples show a small but significant negative Eu anomaly. Most samples when normalized to the Post Archean Australian Shale (Fig. 6; Taylor and McLennan, 1985) or to the continental upper-crust (Supplementary file 1; Taylor and McLennan, 1985), show a relatively uniform pattern for REEs with only some differences in relative abundance. However, Samples ST-DZ 1, 3, 4 and 5 exhibit a significantly different pattern. San Pedro Formation ironstones (ST-DZ1 and ST-DZ3) have higher values of HREE, Olleros Formation (ST-DZ4) has lower values of LREE, whereas Ermita Formation (ST-DZ5) contains low amounts of REE in general.

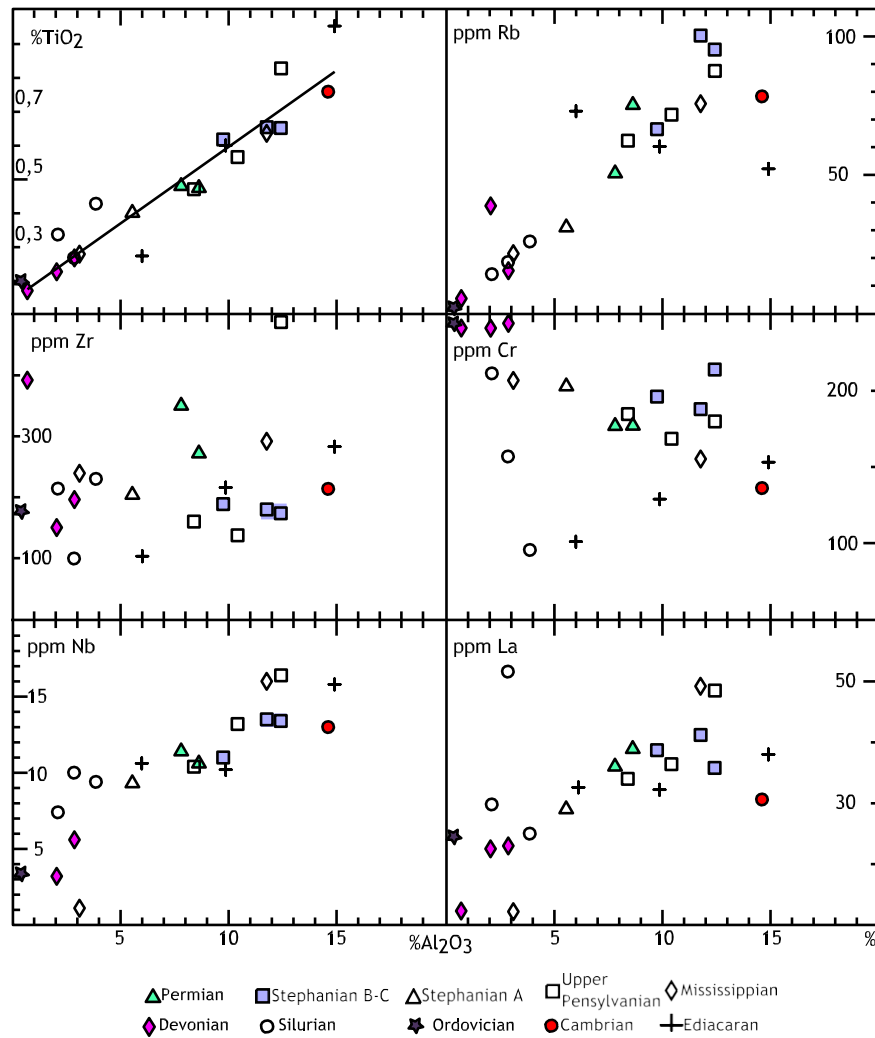


Fig. 4. Variation diagrams of Al_2O_3 vs. TiO_2 (wt.%), Rb, Nb, Cr, Zr and La (ppm). See text for explanation and discussion.

In common tectonic discrimination diagrams (Fig. 7) Ediacaran rocks plot typically in the Continental Island Arc field or the Oceanic Island Arc field whereas, Cambrian sample (OD1) plots both in island arc and passive margin settings (see Fernández-Suárez et al., in press) and Ordovician to Devonian samples plot predominantly in the passive margin field. There are exceptions to these generalities; a Silurian sample (PG14) plots in the active margin field in Fig. 7A, and one Ediacaran sample (OD3) plots in the passive margin area in Fig. 7E. Carboniferous and Permian samples plot adjacent to the boundary between the continental active margin and passive margin fields. Those that plot in the passive margin field lie closer to the active margin field compared to Ordovician to Devonian samples (Fig. 7). San Pedro Formation (ironstones) samples (ST-DZ1 and ST-DZ3) show an anomalous behavior, especially in diagrams that include iron oxides. They fall usually out of the indicated fields or even off the diagram (ST-D3 in diagrams B, C; both in diagram E).

4.2. Sm/Nd isotopic systematics

Sm and Nd are light REE elements that behave coherently in the crust so that the ratio of samarium to neodymium (Sm/Nd) is seldom affected by crustal processes such as anatexis, regional metamorphism, or weathering (Murphy and Nance, 2002). Instead, variations in Sm/Nd in crustal rocks are largely inherited from the depleted mantle, which

preferentially retains samarium over neodymium (DePaolo, 1981; DePaolo and Wasserburg, 1976; McCulloch and Wasserburg, 1978). The Sm/Nd isotopic signature is therefore useful to constrain the provenance of low grade clastic rocks (Murphy and Nance, 2002) as it is the case of the Cantabrian Zone (see Section 2).

The ϵ_{Nd} values (Table 2) were calculated using a $^{143}\text{Nd}/^{144}\text{Nd} = 0.512638$ value for the present day chondrite uniform reservoir (CHUR) and are given as present-day values and also as values calculated to the depositional age of the rocks. ^{147}Sm decay constant is $6.54 \times 10^{-12} \text{ y}^{-1}$ (Steiger and Jager, 1978). T_{DM} values (Table 2) were calculated with respect to the De Paolo mantle model (DePaolo, 1981, 1988) for the depositional age of the studied rocks.

Fig. 8 and Table 3 show the results obtained. Depositional ages (from Bastida, 2004) are as shown in Table 1. As comparison between samples of various depositional ages is visually simplified by comparing their $\epsilon_{\text{Nd}(0)}$ values at the same age, we compare their present-day values (i.e. $\epsilon_{\text{Nd}(0)}$) and their T_{DM} ages. Ediacaran rocks have $\epsilon_{\text{Nd}(0)}$ values around -8.5 , the Cambrian sample has a value of -16.8 , whereas Ordovician to Permian rocks range from -10.1 to -14.3 . T_{DM} ages can be classified into four different groups: (i) Ediacaran rocks that have T_{DM} ages about 1.35 Ga; (ii) Cambrian sample with a T_{DM} age of 1.9 Ga; (iii) pre-Variscan samples with T_{DM} ages ranging from 1.9 to 2.14 Ga; and (iv) syn- and post-Variscan samples which have T_{DM} ages ranging from 1.45 to 2.0 Ga with younger rocks trending toward

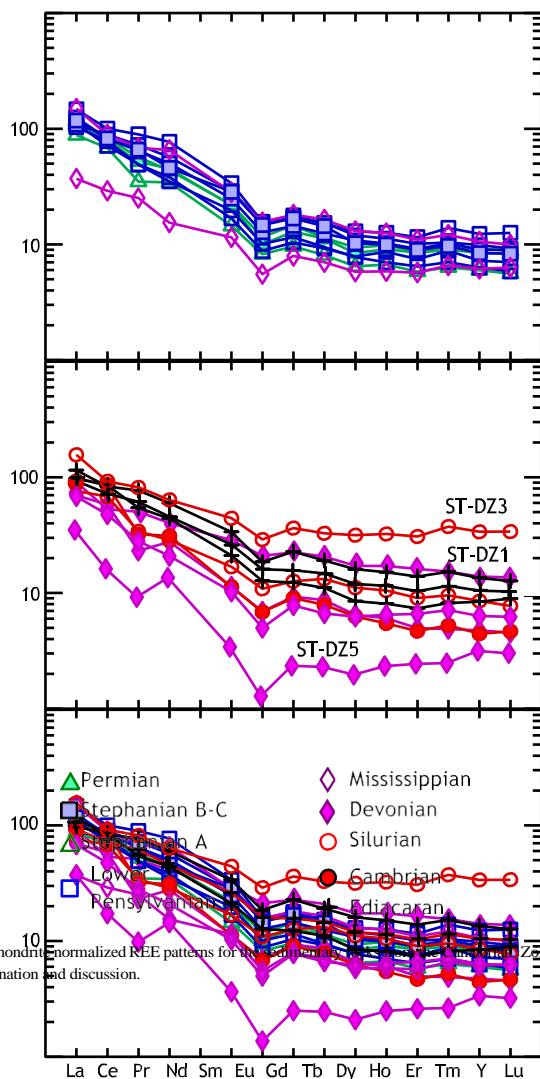


Fig. 5. Chondrite-normalized REE patterns for the sedimentary rocks from the Cantabrian Zone. See text for explanation and discussion.

younger T_{DM} ages (Table 3). A transition from a more juvenile signal in the Neoproterozoic to a cratonic-like signal in Cambrian is also observed on the African margin of Gondwana through Sm–Nd and U–Pb–Hf isotopic relationships (Avigad et al., 2012; Ugidos et al., 1997, 2003; Valladares et al., 2002) and has been interpreted by the mentioned authors as either the erosion of deeper crustal levels in an age-ordered upper crust or the provenance change due to the end of the Neoproterozoic subduction related magmatism.

4.3. X-ray diffraction

Kubler Index (KI) is highly variable due to the sum in the 10\AA peak of variable quantities of crystalline detrital mica and R3 I/S mixed-layer, showing partially variable proportions of illitic layers and consequently d spacing. The significant presence of detrital mica in the samples and its

effect on the measure is evident by the systematic difference in values obtained on the whole fraction in relation to those of the $b\text{-}2\text{-}\mu\text{m}$ fraction (Fig. 2; Table 4). When the samples are EGC solvated, the treatment affects the position of the mixed-layer peak due to the swelling of their smectitic layers, producing lower KI than in the non-treated samples. Also the KI measured on the 5\AA peak yields lower values than those of the 10\AA , due to the clearly different relative contributions of mixed-layers and detrital micas on the two peaks (Nieto and Sanchez-Navas, 1994). In any case, most of the samples have KI values in the range corresponding to diagenetic conditions. X-ray diffraction studies (Table 4) indicate that the mineral composition of most samples is dominated by mica, chlorite, and kaolinite. Former smectite has been completely transformed in a mature illite/smectite mixed-layer of the R3 type, with at least 90% illite layers. All the samples (Fig. 2; Table 4) reached deep diagenetic conditions with the exception of the Stephanian B–C post-Variscan samples (PG7, PG8 and PG11) that reached lower anchizone conditions. Even if samples PG7 and PG11 present a low quantity of kaolinite, we can keep their assignment to anchizone or the limit diagenesis–anchizone, given by the Kubler Index, as right; their small quantity of kaolinite could be a non-equilibrated rest of the former diagenetic conditions or the effect of retrograde processes previously described by Frings and Warr (2012) in similar samples from the Cifra-Matallana basin. In general, crystallinity is higher in Stephanian B–C samples and the syn-orogenic Bashkirian–Moscowian strata (PG4, PG5 and PG6). These data are consistent with previous analyses in the Cantabrian Zone in which more crystalline KI values are found in locations around the Leon breaching thrust (Alonso et al., 2009; Bastida et al., 2004; Frings and Warr, 2012; García-López et al., 2007) and in the Narcea Antiform (García-López et al., 2007; Gutiérrez-Alonso and Nieto, 1996 and references therein).

4.4. Compilation of detrital zircon geochronology

In recent years, studies utilizing U–Pb detrital zircon age populations of clastic sedimentary rocks have enabled the investigation of processes such as exhumation rates and related changes in topography during major tectonic events (Lonergan and Johnson, 1998; Nie et al., 2010; Stewart et al., 2008; Weislogel et al., 2010). Several provenance studies have focused on the Ediacaran to Permian sedimentary rocks from the W Iberian Variscides (e.g. Martínez et al., 2008; Pastor-Galán et al., 2013; Pereira et al., 2012) in order to understand the paleogeographic evolution of the northern Gondwana margin mainly during Ediacaran and Early Paleozoic times (e.g. Díez-Fernández et al., 2010; Fernández-Suárez et al., 1999, 2000; Fernández-Suárez et al., 2002, in press; Gutiérrez-Alonso et al., 2003; Catalan et al., 2004).

We compiled the published data from the Cantabrian Zone (Fernández-Suárez et al., 2002, in press; Pastor-Galán et al., 2013; Shaw et al., in press) in order to complement the geochemical and Sm–Nd data presented in this study and to facilitate an examination of the tectonic evolution of the Gondwanan foreland from late Ediacaran to Early Permian times.

For this purpose we use the method of Cawood et al. (in press; Fig. 9) that discriminates tectonic setting by subtracting the depositional age of a sedimentary rock from every detrital zircon age in the data set for that sample. The ages obtained are then plotted on a cumulative frequency diagram. Fig. 9 shows such a plot constructed using the detrital U–Pb age data taken from the following sample sets: Ediacaran (OD2, OD5 and OD7) and Cambrian sample (OD1) from Fernández-Suárez et al. (in press); Ordovician (Fernández-Suárez et al., 2002; Shaw et al., in press); Silurian (PG14: Pastor-Galán et al., 2013); Devonian (ST-DZ1 and PG12 from Pastor-Galán et al., 2013 respectively); Pennsylvanian (PG4, PG5, PG6, PG9, ST-DZ4); post-orogenic Stephanian (PG1, PG7, PG8, PG11) and Early Permian (PG2, PG3). Pennsylvanian to Early Permian data are from Pastor-Galán et al. (2013).

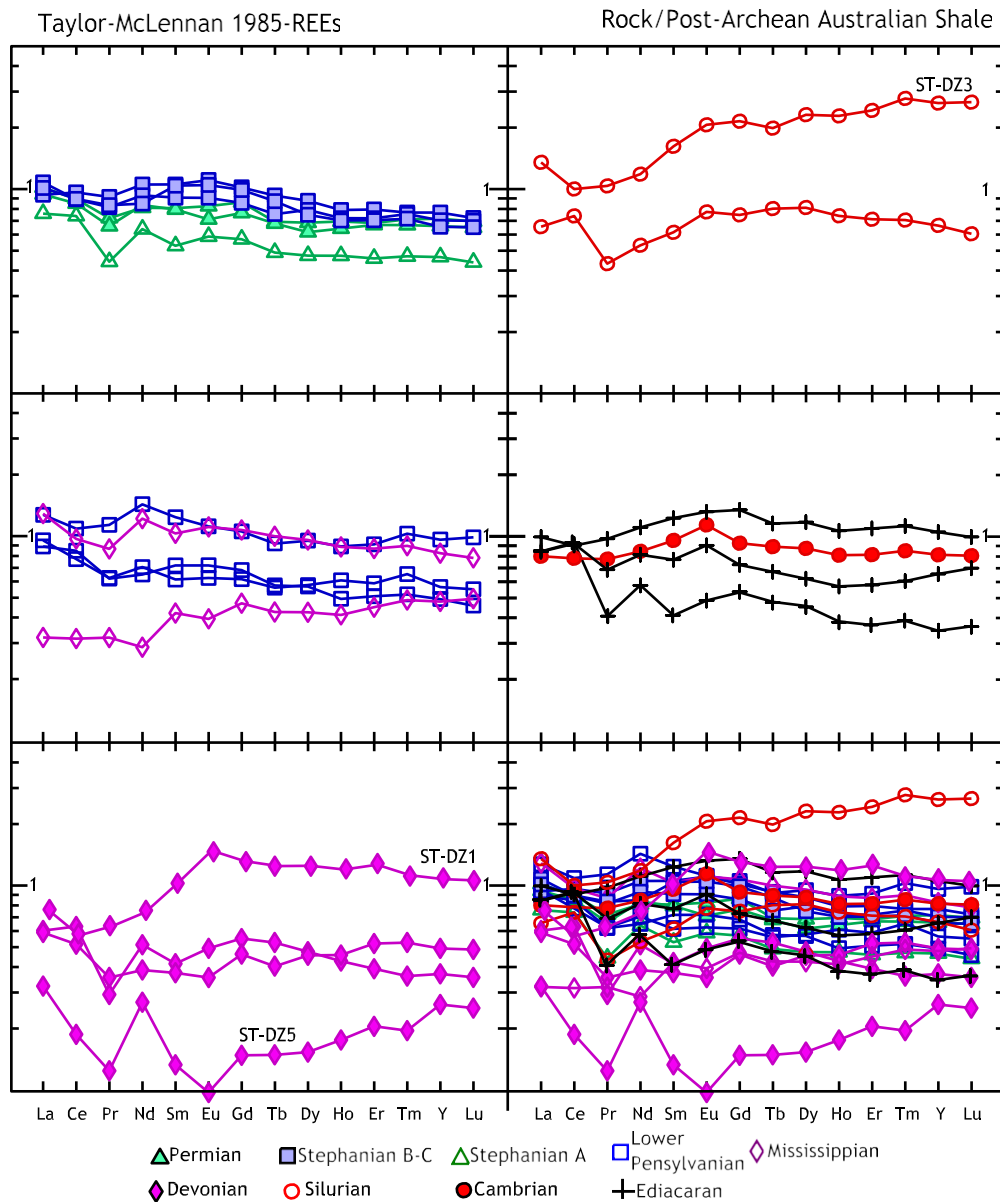


Fig. 6. PAAS normalized (after Taylor and McLennan, 1985) REE patterns for the sedimentary rocks from the Cantabrian Zone. See text for explanation and discussion.

Detrital zircon age distribution plots (Fig. 9) support inferences based on the lithochemical data and suggest that Ediacaran samples were formed in a magmatic arc setting. Cambrian sample OD1 still meets the requirements of active settings (crystallization age–depositional age values at 5% and 30% fit well with active margin setting), although its cumulative frequency curve is very different to that of the Ediacaran samples owing to the high proportion of Paleoproterozoic zircons and the absence of the 0.8–1.1 population (Fernández-Suárez et al., in press). The rest of the samples plot in the overlapping space for passive-margin and collisional setting. However it is noticeable that pre-Variscan rocks (in blue) plot closer to the passive-margin whereas syn- and post-Variscan rocks (green and red) plot closer to the collisional setting.

5. Discussion

As described in the Introduction, a variety of different tectonic and paleogeographic models have been proposed for the Paleozoic

evolution of NW Iberia. In this section of the paper, we give a step-by-step interpretation of the new data and combine it with data from the literature in order to give an overall interpretation of evolution of NW Iberia during the Paleozoic.

5.1. Significance of whole rock geochemical data

Geochemistry of clastic strata in the Cantabrian Zone shows, in general, an upper crust composition (McLennan, 2001; Taylor and McLennan, 1985). Samples show a good correlation of SiO_2 and Al_2O_3 , with other major and minor components (Figs. 3 and 4), suggesting that the main differences in major and minor elements are a function of the relative abundance of quartz and the mica/clay fraction, and therefore sorting. Positive correlation of Cr and SiO_2 suggests a linkage between Cr and quartz. The lack of correlation between Zr and SiO_2 or Al_2O_3 , together with the strong correlation between Zr and Hf, and the positive correlation found with compatible REE suggest that most of the Zr come from zircons. The geochemistry of the San Pedro Formation

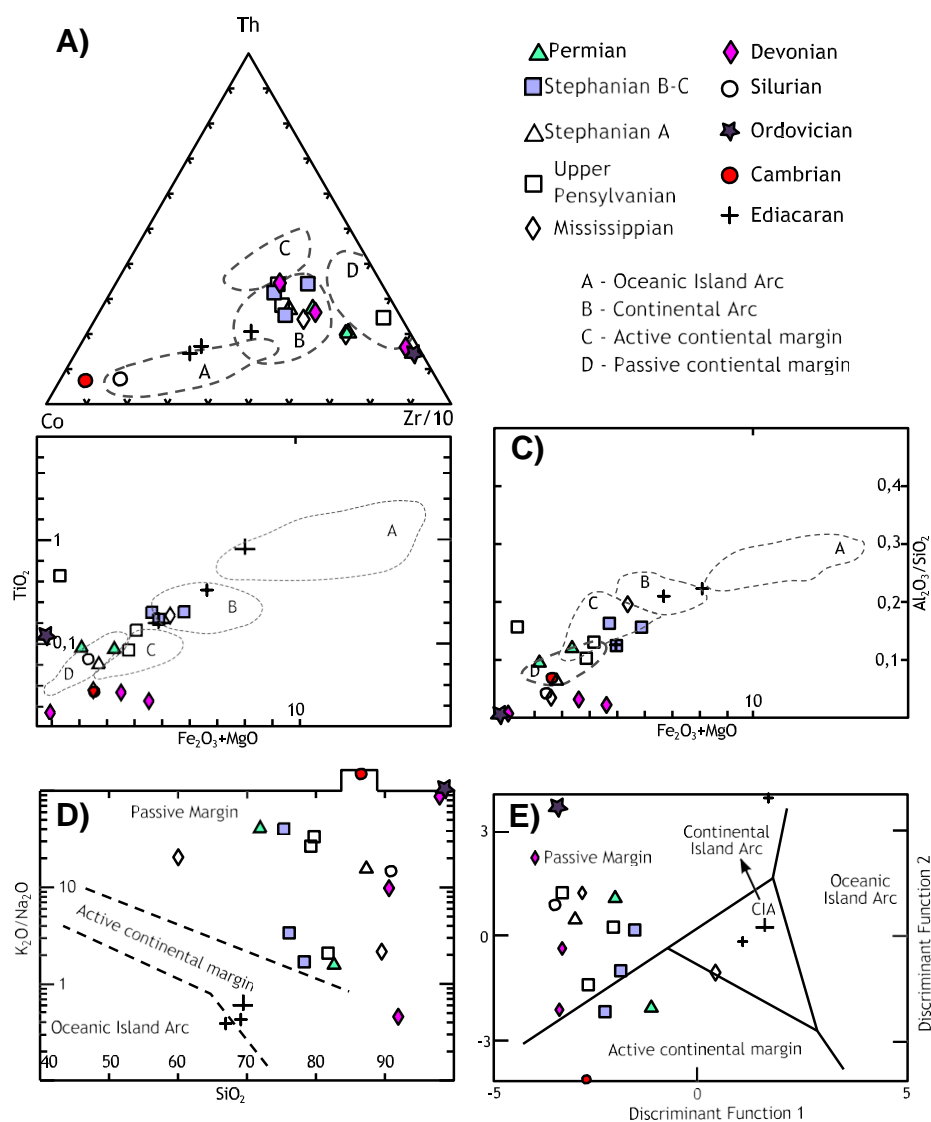


Fig. 7. Discrimination diagrams for the Cantabrian Zone rocks. A) Co-Th-Zr/10 diagram after Taylor and McLennan (1985). B) TiO_2 vs. Fe_2O_3+MgO and C) Al_2O_3/SiO_2 vs. Fe_2O_3+MgO both after Bathia (1983). D) K_2O/Na_2O vs. SiO_2 after Roser and Korsch (1986). E) Discriminant function diagram of Bathia (1983).

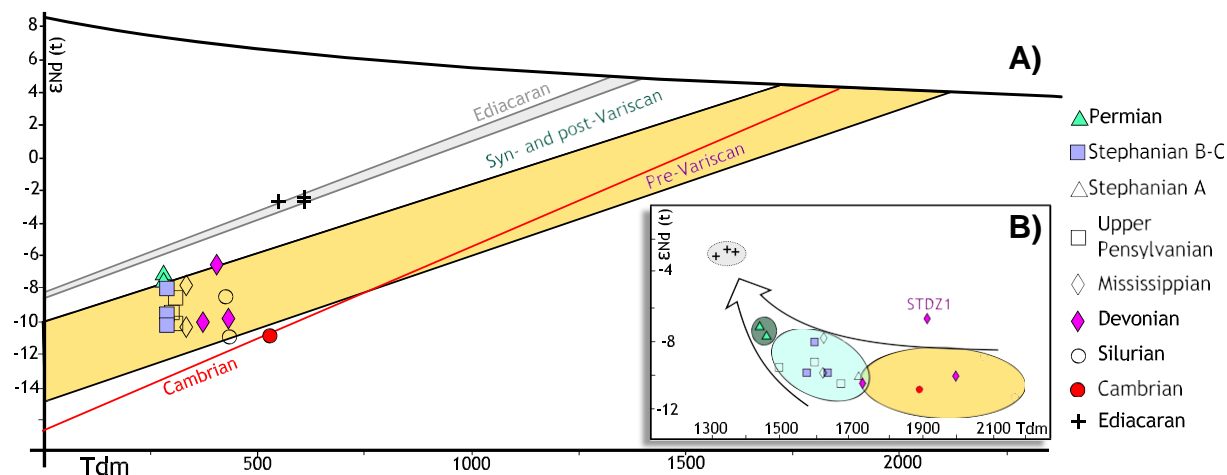


Fig. 8. A) $\epsilon Nd(t)$ vs. age (DePaolo, 1981) for the Cantabrian Zone samples. B) $\epsilon Nd(t)$ vs. T_{DM} diagram (see text for discussion).

Table 3
Sm-Nd analytical results of the samples in this study.

| | Nd (ppm) | Sm (ppm) | $^{147}\text{Sm}/^{144}\text{Nd}$ | $^{143}\text{Nd}/^{144}\text{Nd}$ | 2 σ | Epsilon (0) | Epsilon (350) | Epsilon (600) | Epsilon (form) | T De Paolo | TDM2 |
|-------|----------|----------|-----------------------------------|-----------------------------------|------------|-------------|---------------|---------------|----------------|------------|--------|
| OD-1 | 15.9 | 2.9 | 0.1 | 0.5 | 7.0 | -16.8 | -13.0 | -10.3 | -10.9 | 1889.0 | 2044.5 |
| OD-2 | 29.6 | 5.7 | 0.1 | 0.5 | 7.0 | -8.4 | -4.9 | -2.4 | -3.0 | 1325.0 | 1496.2 |
| OD-5 | 28.0 | 5.5 | 0.1 | 0.5 | 7.0 | -8.6 | -5.2 | -2.7 | -2.7 | 1361.0 | 1534.2 |
| OD-7 | 36.3 | 7.2 | 0.1 | 0.5 | 7.0 | -8.6 | -5.2 | -2.7 | -2.7 | 1377.0 | 1552.3 |
| PG-1 | 17.7 | 3.4 | 0.1 | 0.5 | 7.0 | -13.3 | -9.8 | -7.2 | -10.2 | 1719.0 | 1888.5 |
| PG-2 | 23.2 | 4.4 | 0.1 | 0.5 | 7.0 | -10.7 | -7.0 | -4.4 | -7.7 | 1463.0 | 1630.1 |
| PG-3 | 24.2 | 4.7 | 0.1 | 0.5 | 7.0 | -10.1 | -6.5 | -4.0 | -7.2 | 1446.0 | 1616.6 |
| PG-4 | 20.6 | 3.5 | 0.1 | 0.5 | 7.0 | -13.2 | -9.1 | -6.1 | -9.5 | 1501.0 | 1650.0 |
| PG-5 | 22.7 | 4.3 | 0.1 | 0.5 | 7.0 | -12.6 | -8.9 | -6.2 | -9.2 | 1593.0 | 1757.4 |
| PG-6 | 62.1 | 11.6 | 0.1 | 0.5 | 7.0 | -13.7 | -9.9 | -7.3 | -10.4 | 1667.0 | 1828.7 |
| PG-7 | 32.7 | 6.1 | 0.1 | 0.5 | 8.0 | -13.2 | -9.5 | -6.8 | -10.0 | 1630.0 | 1791.0 |
| PG-8 | 26.4 | 4.8 | 0.1 | 0.5 | 6.0 | -13.3 | -9.4 | -6.6 | -9.9 | 1577.0 | 1733.9 |
| PG-9 | 29.4 | 5.7 | 0.1 | 0.5 | 7.0 | -13.7 | -10.1 | -7.6 | -10.5 | 1736.0 | 1903.8 |
| PG-11 | 31.2 | 6.2 | 0.1 | 0.5 | 6.0 | -11.1 | -7.8 | -5.3 | -8.2 | 1599.0 | 1776.0 |
| PG-12 | 12.2 | 2.6 | 0.1 | 0.5 | 7.0 | -13.2 | -10.3 | -8.2 | -10.1 | 1993.0 | 2185.3 |
| PG-14 | 19.2 | 4.2 | 0.1 | 0.5 | 8.0 | -14.8 | -11.9 | -9.8 | -11.2 | 2146.0 | 2334.9 |
| STDZ5 | 5.1 | 0.9 | 0.1 | 0.5 | 9.0 | -11.6 | -7.5 | -4.7 | -7.3 | 1414.0 | 1566.6 |
| STDZ2 | 13.7 | 2.5 | 0.1 | 0.5 | 9.0 | -14.3 | -10.3 | -7.5 | -9.8 | 1633.0 | 1787.6 |
| STDZ1 | 26.0 | 6.1 | 0.1 | 0.5 | 5.0 | -9.5 | -7.1 | -5.4 | -6.7 | 1915.0 | 2145.4 |
| STDZ3 | 40.5 | 9.3 | 0.1 | 0.5 | 7.0 | -12.0 | -9.4 | -7.5 | -8.9 | 2067.0 | 2277.5 |
| STDZ4 | 11.2 | 2.3 | 0.1 | 0.5 | 6.0 | -10.8 | -7.6 | -5.2 | -7.8 | 1624.0 | 1806.4 |

(ST-DZ3 and ST-DZ1: Fig. 2) ironstones is different from the other clastic rocks, which we attribute to the significant non-clastic component of these rocks. Its chemical composition is, however, similar to other Paleozoic oolitic ironstones in France (Gloaguen et al., 2007) and Northern Africa (Guerrak, 1987a,b).

Although discrimination diagrams must be used with caution, they do help to identify some broad trends. Ediacaran samples (OD2, OD5 and OD7) plot in the fields of Oceanic or Continental island arcs consistent with previous interpretations of the Narcea Slates as backarc basin deposits (e.g. Fernández-Suárez et al., 1998; Gutiérrez-Alonso et al., 2005) and with NW Iberia as part of an arc system during the Late Neoproterozoic (e.g. Murphy et al., 2006; Fuenlabrada et al., 2012; Fernández-Suárez et al., in press). We interpret the ambiguity of Cambrian sample (OD1) as result of the transition from the Neoproterozoic island-arc setting to the extension and platform development during the opening of the Rheic Ocean. This interpretation is supported by geochemical data, Sm/Nd isotopes and U/Pb geochronology in detrital zircons in other Cambrian rocks in NW Iberia out of the Cantabrian Zone (Fernández-Suárez et al., in press). Following these authors slightly older Early Cambrian samples out of the Cantabrian Zone show a major and trace element geochemistry consistent with an active

continental margin. The Cambrian sample from the Cantabrian Zone (OD1) show lower amounts of FeO, MgO and TiO₂ and higher SiO₂ which is akin to passive-margin conditions.

Ordovician to Devonian samples plot in the passive margin field whereas Carboniferous and Permian samples plot either in the active continental margin field or close to it (Fig. 7). This pattern suggests a relatively stable source of sediment for the Cantabrian Zone, (presumably from the Gondwanan margin) from the Ordovician to the Devonian. Recycling of these strata occurred during the Variscan orogeny when the Cantabrian Zone was a foreland basin (Late Mississippian) and also during subsequent oroclinal buckling (e.g. Pastor-Galán et al., 2013; Weil et al., 2013 and references therein).

REE patterns in most clastic sedimentary rocks are similar to Post-Archean Australian Shale (PAAS), considered an average for terrigenous contributions (Taylor and McLennan, 1985). The only samples that do not present an almost parallel pattern to the PAAS are the Ediacaran samples (OD2, OD5 and OD7), the San Pedro formation (ST-DZ1 and ST-DZ3), and Ermita formation (ST-DZ5) whose content in REE is so low that comparisons may not be representative (Figs. 5 and 6; Tables 1 and 2). We argue that the differences observed in the Ediacaran samples respond to the immaturity of the sediment which in turn may

Table 4
X-ray diffraction data for the rocks of the Cantabrian Zone. Legend: quartz (Qtz), smectite (Sme), plagioclase (Pl), chlorite (Chl), kaolinite (Kln), calcite (Cal), dolomite (Dol), – scarce, +abundant.

| | Mineral composition | b2 μ | EG | Total | b2 μ 5 Å | b2 μ | | Total | |
|-------|--|----------|------|-------|--------------|----------------------|-----------------------|----------------------|-----------------------|
| | | | | | | d ₀₀₁ cta | d ₀₀₁ mica | d ₀₀₁ cta | d ₀₀₁ mica |
| PG 1 | Qtz, Mica, Kln, Cal, Sme, Int (R3) | 1.10 | 0.77 | 1.00 | 0.65 | — | — | — | 9.986 |
| PG 2 | Qtz, Mica, Kln, Cal, Sme, Int (R3) | 0.92 | 0.70 | 0.81 | 0.53 | — | 9.990 | — | 9.990 |
| PG 3 | Qtz, Mica, Kln, Cal, Sme, Int (R3), Pl | 0.79 | 0.58 | 0.46 | — | — | — | — | 9.986 |
| PG 4 | Qtz, Mica, Kln, Int (R3), Pl | 0.79 | 0.39 | 0.20 | 0.52 | — | 9.986 | — | 9.980 |
| PG 5 | Qtz, Mica, Chl, Kln-, Int (R3), Pl | 0.52 | 0.42 | 0.31 | 0.44 | 14.12 | 9.985 | 14.12 | 9.981 |
| PG 6 | Qtz, Mica, Kln, Int (R3), Pl- | 0.58 | 0.45 | 0.23 | 0.41 | — | 9.987 | — | 9.979 |
| PG 7 | Qtz, Mica, Chl, Kln-, Int (R3), Pl | 0.42 | 0.39 | 0.24 | 0.37 | 14.13 | 9.994 | 14.12 | 9.989 |
| PG 8 | Qtz, Mica, Chl, Pl- | 0.36 | 0.40 | 0.32 | 0.34 | 14.12 | 9.991 | 14.12 | 9.984 |
| PG 9 | Qtz, Mica, Kln, Cal, Dol, Int (R3) | 1.20 | 0.69 | 0.76 | 0.60 | — | 9.998 | — | — |
| PG 10 | Qtz, Mica, Chl, Int (R3) | 1.08 | 0.64 | — | — | 14.11 | — | 14.11 | — |
| PG 11 | Qtz, Mica, Chl, Kln, Int (R3), Pl | 0.35 | 0.32 | 0.21 | 0.32 | 14.14 | 9.970 | 14.14 | 9.970 |
| PG 12 | Qtz+, Mica, Kln-, Int (R3) | 1.03 | 1.16 | — | — | — | — | 14.14 | 9.979 |
| PG 13 | Qtz, Mica, Chl, Int (R3), Pl | 0.98 | 0.64 | 0.35 | 0.52 | 14.14 | 9.979 | 14.13 | — |
| PG 14 | Qtz+, Mica, Chl, Int (R3), | 0.92 | 0.93 | 0.83 | 0.58 | 14.13 | — | 14.12 | — |

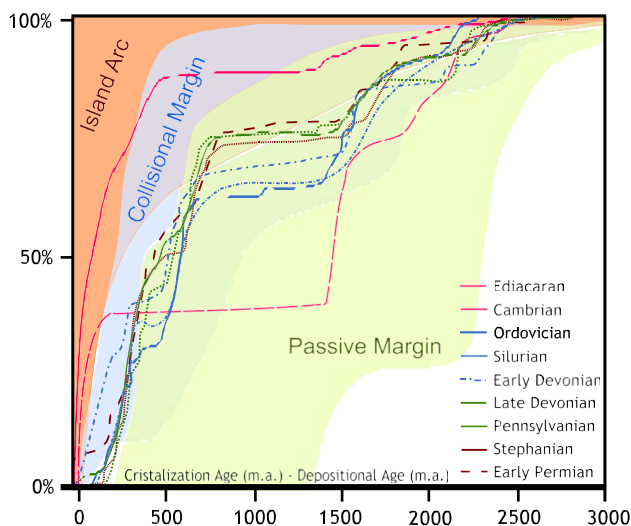


Fig. 9. Discrimination diagram of Cawood et al. (in press) which is an accumulative diagram plotting crystallization age–depositional, for illustration of the tectonic environment of deposition of the studied rocks (see text for details).

reflect its back-arc basin tectonic setting (e.g. Gutiérrez-Alonso et al., 2005).

The origin of the San Pedro Fm ironstones is enigmatic. Van Houten and Arthur (1989) and Van Houten (1990) emphasized that oolitic ironstones accumulate during certain intervals of relatively high sea level, declining tectonic activity, and after deposition of black shales. It is an observation that oolitic ironstones are widespread during time intervals that record this sequence of conditions (McLaughlin et al., 2012; Taylor et al., 2002). Sedimentary ironstones are extensive worldwide in Lower Silurian and Early Devonian (e.g. Guerrak, 1987a,b; Van Houten and Arthur, 1989; Van Houten, 1990). Additionally, in the case of the Cantabrian Zone, the Silurian Formigoso black shales underlie the San Pedro Fm. Therefore, it is conceivable that an intra-Rheic or even a global event took place that changed the redox conditions of the ocean(s) likely related with a biogenic event (Brett et al., 2012; Ferretti et al., 2012).

5.2. Significance of Sm/Nd isotope systematics

The Nd isotopic signature in clastic rocks represents the weighted average of the detrital contributions from their source areas (e.g. Murphy and Nance, 2002). The Ediacaran samples have the youngest T_{DM} model ages and less negative ϵ_{Nd} values. This is consistent with a more juvenile input in the suggested back-arc setting where these rocks were deposited. In the Paleozoic rocks, the limited variations both in $\epsilon_{Nd(t)}$ and T_{DM} imply that the source of sediment was broadly similar from Ordovician to Permian, either because they share the same source or because of the recycling of clastic rocks due to the Variscan orogenesis. This slight dissimilarity in Sm–Nd isotopic signature is consistent with the pattern defined by major, trace and REE elements, i.e. a passive margin that evolves into a foreland basin fed by the passive margin previously deposited rocks. However, syn- and post-Variscan samples have younger T_{DM} model ages, a trend which is shown clearly in the $\epsilon_{Nd(t)}$ vs. T_{DM} plot (Fig. 8B). We attribute the younger T_{DM} model ages observed in the Carboniferous samples to the erosion of the Variscan orogen that included the uplifted volcanic complexes (The “Ollo de Sapo” and other related Ordovician mafic rocks e.g. Díez Montes, 2006; Gutiérrez-Alonso et al., 2011a; Murphy et al., 2008 which has a T_{DM} between 0.9 and 1.1 Ga), an observation that is consistent with the presence of detrital zircon ages from 500 to 470 found in the syn-Variscan samples (Pastor-Galán et al., 2013).

Permian strata are interbedded with volcanics that are interpreted to have been generated as a consequence of lithospheric foundering (T_{DM} of the volcanics is younger than 1.0 Ga; e.g. Gutiérrez-Alonso et al., 2011a,b). The clastic rock itself (PG2 and PG3) contains zircons with the same age as the deposition age (Pastor-Galán et al., 2013). We consider the additional presence of this relatively juvenile source to be the responsible of the relatively young T_{DM} ages of Permian clastic rocks.

In summary, Sm/Nd isotopic systematics support the notion that NW Iberia had a stable source of sediments from Ordovician to Devonian times followed by recycling of strata during the Carboniferous Variscan orogenesis. In Permian times a younging of T_{DM} ages reflects basin formation related with the post-orogenic uplift of the Cantabrian Zone likely produced by mantle–lithosphere foundering (Pastor-Galán et al., 2013).

Another insight derived from the Sm/Nd systematics in the studied rocks affects the interpreted origin of the Siluro-Devonian ironstones of the San Pedro Formation. As stated before, this formation can be interpreted as deposited in a passive margin during a low sedimentation rate period, but previous studies have claimed that the origin of the ironstones is derived from a coeval volcanic activity (Suárez de Centi, 1988). According to our results, if this formation had a substantial volcanic input its Sm/Nd signature should be comparably more juvenile than the other sedimentary rocks deposited in the same continental margin, which is not the case. From this point of view we can assume an origin for the ironstones in agreement with the data described before and that there is no need to invoke a volcanic event at that time.

5.3. Significance of the illite crystallinity data

All samples have a mineral assemblage typical of deep diagenetic conditions, a result that is consistent with previous data (e.g. Abad et al., 2003, 2006; García-López et al., 2007; Gutiérrez-Alonso and Nieto, 1996). This implies that there is no record of a significant metamorphic event during the Neoproterozoic and Paleozoic in the CZ (Gutiérrez-Alonso and Nieto, 1996). However, the syn-orogenic samples and the Stephanian BC samples have values of KI close to the low anchizone conditions (PG7, PG8 and PG11). These results compare well with reflectance of vitrinite obtained in coal ranks in the Cantabrian Zone (Colmenero et al., 2008). This relatively high grade may be attributed to fluid-driven processes responsible for, among other features, the widespread dolomitization (e.g. Gasparini et al., 2003, 2006) and gold mineralization (Martin-Izard et al., 2000) in the CZ. Recently, Frings and Warr (2012) have related anchizone grades, reached by Stephanian samples in areas of high heat and fluid flow of the Cíñera-Matallana basin, with localized igneous and hydrothermal activity associated with syn-orocline buckling strike-slip-faulting.

5.4. Tectonic setting implied by detrital zircons

The detrital zircon age distribution in relation to depositional age (Fig. 9) supports a magmatic arc setting for the Ediacaran samples, and a relatively stable source of zircons from Ordovician to Permian.

Cambrian sample (OD1) seems to be quite exceptional because of the absence of 1000 m.a. population. In any case, the first 20% of the zircons indicate active margin conditions which reinforces the ambiguity of the sample. Other slightly older Early-Cambrian samples in NW Iberia located out of the Cantabrian Zone show typical characteristics of an active margin (Fernández-Suárez et al., in press). The difference between them may imply changes in the drainage system or local source areas in the Cantabrian Zone at that time, maybe indicating the transitional geodynamic regime during Cambrian times in northern Gondwana.

Pre-Variscan samples plot closer to the passive-margin setting and syn- and post-Variscan samples plot closer to the collisional setting reflecting the input of younger zircons. Following Pastor-Galán et al. (2013), the syn-Variscan and post-Variscan strata contain detritus that

were recycled from rocks formed previously in the Gondwana margin including some input from igneous bodies related with the opening of the Rheic and syn-orogenic (Variscan) igneous rocks, which explains why syn- and post-Variscan strata have a similar detrital zircon record.

5.5. Paleozoic evolution of NW Iberia

Although it is widely accepted that some microcontinents (e.g. Avalonia, Carolina, Meguma, Ganderia) drifted away from Gondwana during the Ordovician (Nance et al., 2010 and references therein), there is still a strong discussion about the possible separation of the Armorica/Galatia terranes during the Late-Silurian–Devonian (Stampfli et al., 2013 and references therein). The geochemical record

of the Cantabrian Zone presented in this paper, together with structural geology, detrital geochronology and sedimentology sheds light on this controversy.

Fig. 10 is a synthesis of the tectonic evolution of the NW margin of Iberia from Ediacaran to Early Permian times using data from this paper and data available from the literature. All of these data suggest that NW Iberia evolved from a Neoproterozoic arc setting through a rifting stage during the Late Cambrian and Early Ordovician being the Cambrian a period of transition from active margin to rift development. Unfortunately geochemistry, Sm–Nd and detrital zircon record of Ediacaran to Ordovician sedimentary rocks do not help to distinguish whether the transition from back-arc to rift happened due to slab pull (e.g. Murphy et al., 2006) or slab roll-back (e.g. Fuenlabrada et al.,

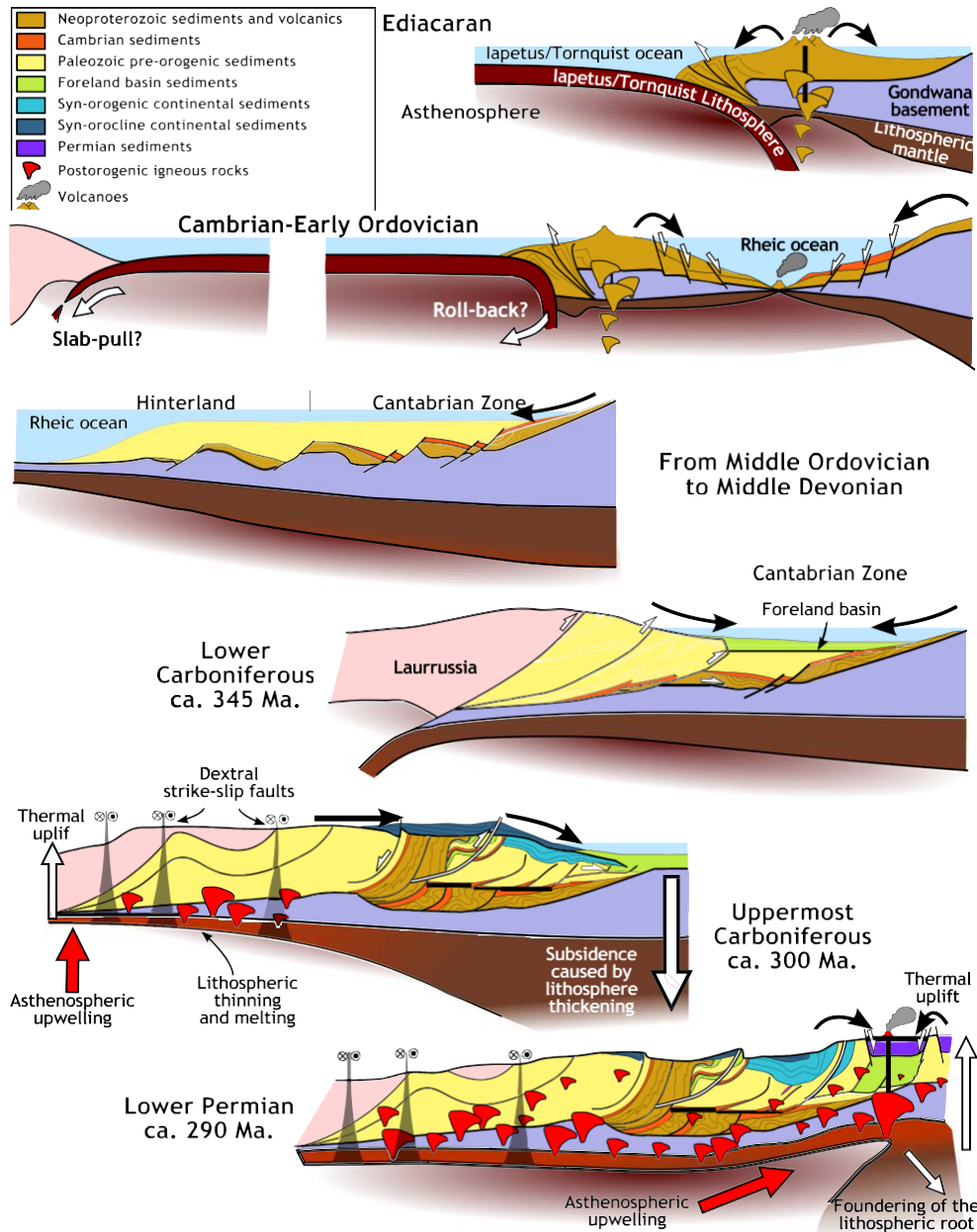


Fig. 10. Synthesis of the proposed tectonic evolution of NW Iberia based on data presented herein as well as previously published data (see references in text). During the Ediacaran, NW Iberia formed part of a back arc basin that evolved to a passive margin during the formation of the Rheic Ocean, in the Late Cambrian and Early Ordovician times. From Ordovician to Middle Devonian times, NW Iberia was part of the passive-margin along the northern Gondwanan margin that received sediments derived from the cratons in the hinterland as well as from recycling of the Ediacaran arc. During most of the Carboniferous the sedimentary basin evolved into a foreland basin receiving sediments from the orogen as well as adjacent cratonic areas. During the Pennsylvanian (Bashkirian–Moskovan), the foreland basin was being deformed and syn-tectonic continental sediments were deposited. After collisional orogenesis ceased, lithospheric scale oroclinal buckling produced sediment discharge directed towards the core of the orocline. At about the Carboniferous–Permian boundary, lithospheric–mantle foundering produced asthenospheric thermal uplift causing melting and thermal uplift. Grabens formed with local sedimentary sources.

2012; Fernández-Suárez et al., 2013). After the rifting, a passive margin developed with a stable source of sediments from Gondwana continent during most of the Paleozoic followed by a Late Paleozoic active margin development (Fig. 10). Neither geochemistry, nor Sm–Nd systematics support the opening of a back-arc basin to the south (in Paleozoic coordinates) of the Cantabrian zone or to the core of the Cantabrian Arc (in present day coordinates) (e.g. Tait et al., 1994; Torsvik and Cocks, 2004; Van Der Voo, 1982, 1993) nor the onset of a subduction zone southwards (Stampfli and Borel, 2002) or northwards (Stampfli et al., 2013) as would be implied by separation of Armorica/Galatia terranes during Late Silurian–Devonian. From this point of view it is difficult to argue the presence of NW Iberia in the alleged ribbon continent (Armorica–Galatia–ATA) as the processes involved in its generation (rifting from the northern Gondwana margin) and subsequent re-amalgamation (subduction related to the closure of the newly formed ocean) would have left its geochemical and isotopic imprint in the studied sediments.

6. Conclusions

Whole rock geochemistry, Sm–Nd systematics and X-ray diffraction data presented herein suggest that NW Iberia was an active margin during the Ediacaran that evolved to a rift basin during Late Cambrian and Early Ordovician, either due to slab-pull (Murphy et al., 2006) or to subduction zone roll-back (e.g. Díez Fernández et al., 2012). After the generation of the Rheic Ocean, NW Iberia remained a passive margin until the Late Devonian without evidence of the generation of a ribbon continent that would lead to the opening of a new ocean located in the core of the nowadays Cantabrian Orocline. Data from Carboniferous and Permian strata record the evolution from a passive to an active margin coincident with the development of the Variscan orogeny and the post-Variscan oroclinal buckling. The Sm–Nd systematics and X-ray diffraction also record a thermal event in that affected the Uppermost Carboniferous rocks. We interpret this event to be a consequence of the lithospheric foundering that occurred in Early Permian following Late Carboniferous lithospheric thickening that was the result of oroclinal buckling of the Variscan Orogen.

Acknowledgments

This work is part of IGCP 574 and IGCP 597 projects from the UNESCO. Research Projects ODRE II (“Oroclines and Delamination: Relations and Effects”) No. CGL2009-1367, from the Spanish Ministry of Science and Innovation, and N.S.E.R.C., Canada funded this research. JFS wishes to acknowledge financial support from project GCL2012-34618 by the Spanish Ministerio de Economía y Competitividad. Critical reviews from Dov Avigad and an anonymous reviewer helped to improve the manuscript.

Appendix A. Supplementary data

Supplementary data associated with this article can be found in the online version, at <http://dx.doi.org/10.1016/j.lithos.2013.09.007>. These data include Google maps of the most important areas described in this article.

References

Abad, I., Nieto, F., Gutiérrez-Alonso, G., 2003. Textural and chemical changes in slate-forming phyllosilicates across the external–internal zones transition in the low-grade metamorphic belt of the NW Iberian Variscan Chain. *Schweizerische Mineralogische Und Petrographische Mitteilungen* 83, 63–80.

Abad, I., Nieto, F., Gutiérrez-Alonso, G., 2006. Illitic substitution in micas of very low-grade metamorphic clastic rocks. *European Journal of Mineralogy* 18, 59–69.

Abad, I., Murphy, J.B., Nieto, F., Gutiérrez-Alonso, G., 2010. Diagenesis to metamorphism transition in an episutural basin: the late Paleozoic St. Mary's Basin, Nova Scotia, Canada. *Canadian Journal of Earth Sciences* 47, 121–135.

Alonso, J.L., 1989. Fold reactivation involving angular unconformable sequences — theoretical analysis and natural examples from the Cantabrian Zone (northwest Spain). *Tectonophysics* 170, 57–77.

Alonso, J.L., Marcos, A., Suárez, A., 2009. Paleogeographic inversion resulting from large out of sequence breaching thrusts: the León Fault (Cantabrian Zone, NW Iberia). A new picture of the external Variscan Thrust Belt in the Ibero-Armorican Arc. *Geologica Acta* 7, 451–473.

Alvarez-Marron, J., Perez-Estaun, A., 1988. Thin skinned tectonics in the Ponga region (Cantabrian Zone, NW Spain). *Geologische Rundschau* 77, 539–550.

Aramburu, C., Truyols, J., Arbizu, M., Méndez Bedia, I., Zamarreño, I., García-Ramos, J.C., Suárez de Centi, C., Valenzuela, M., 2002. El Paleozoico Inferior de la Zona Cantábrica. In: Rabano, I., Gutiérrez-Marco, J.C., Saavedra, J. (Eds.), *El Paleozoico Inferior de Ibero-América*. Universidad de Extremadura, pp. 397–421.

Arenas, R., Martínez Catalán, J.R., 2003. Low-P metamorphism following a Barrovian-type evolution. Complex tectonic controls for a common transition, as deduced in the Mondoñedo thrust sheet (NW Iberian Massif). *Tectonophysics* 365, 143–164.

Arenas, R., Martínez Catalán, J.R., Sánchez Martínez, S., Fernández-Suárez, J., Andonaegui, P., Pearce, J.A., Corfu, F., 2007a. The Vila de Cruces ophiolite: a remnant of the Early Rheic Ocean in the Variscan Suture of Galicia (Northwest Iberian Massif). *Journal of Geology* 115, 129–148.

Arenas, R., Martínez Catalán, J.R., Sánchez Martínez, S., Díaz García, F., Abati, J., Fernández-Suárez, J., Andonaegui, P., Gómez-Barreiro, J., 2007b. Paleozoic ophiolites in the Variscan suture of Galicia (northwest Spain). 4-D framework of continental crust. In: Hatcher Jr., R.D., Carlson, M.P., McBride, J.H., Martínez Catalán, J.R. (Eds.), *Geological Society Memoir*, p. 200.

Armstrong-Altrin, J.S., Verma, S.P., 2005. Critical evaluation of six tectonic setting discrimination diagrams using geochemical data of Neogene sediments from known tectonic settings. *Sedimentary Geology* 177, 115–129.

Avigad, D., Gerdes, A., Morag, N., Bechstadt, T., 2012. Coupled U–Pb–Hf of detrital zircons of Cambrian sandstones from Morocco and Sardinia: implications for provenance and Precambrian crustal evolution of North Africa. *Gondwana Research* 21, 690–703.

Barreiro, J.G., Wijbrans, J.R., Castineiras, P., Catalán, J.R.M., Arenas, R., García, F.D., Abati, J., 2006. Ar-40/Ar-39 laserprobe dating of mylonitic fabrics in a polyorogenic terrane of NW Iberia. *Journal of the Geological Society* 163, 61–73.

Bastida, F., 2004. Zona Cantábrica. In: Vera, J.A. (Ed.), *Geología De España*. SGE-IGME, Madrid, pp. 25–49.

Bastida, F., Blanco-Ferrera, S., García-Lopez, S., Sanz-Lopez, J., Valín, M.L., 2004. Transition from diagenesis to metamorphism in a calcareous tectonic unit of the Iberian Variscan belt (central massif of the Picos de Europa, NW Spain). *Geological Magazine* 141, 617–628.

Bea, F., Montero, P., Talavera, C., Zinger, T., 2006. A revised Ordovician age for the oldest magmatism of Central Iberia U–Pb ion microprobe and LA-ICPMS dating of the Miranda do Douro orthogneiss. *Geology Acta* 4, 395–401.

Bhatia, M.R., 1983. Plate tectonics and geochemical composition of sandstones. *Journal of Geology* 91, 611–627.

Bhatia, M.R., Crook, K.A.W., 1986. Trace element characteristics of graywackes and tectonic setting discrimination of sedimentary basins. *Contributions to Mineralogy and Petrology* 92, 181–193.

Brett, C.E., McLaughlin, P.I., Histon, K., Schindler, E., Ferretti, A., 2012. Time-specific aspects of facies: state of the art, examples, and possible causes. *Palaeogeography, Palaeoclimatology, Palaeoecology* 367–368, 6–18.

Brime, C., García-Lopez, S., Bastida, F., Valín, M.L., Sanz-Lopez, J., Aller, J., 2001. Transition from diagenesis to metamorphism near the front of the Variscan regional metamorphism (Cantabrian Zone, northwestern Spain). *Journal of Geology* 109, 363–379.

Catalán, J.R.M., Fernández-Suárez, J., Jenner, G.A., Belousova, E., Montes, A.D., 2004. Provenance constraints from detrital zircon U–Pb ages in the NW Iberian Massif: implications for Palaeozoic plate configuration and Variscan evolution. *Journal of the Geological Society* 161, 463–476.

Cawood, P.A., Hawkesworth, C.J., Dhuime, B., 2013. The continental record and the generation of continental crust. *Geological Society of America Bulletin* 125, 14–32.

Colmenero, J., Suárez-Ruiz, I., Fernández-Suárez, J., Barba, P., Llorens, T., 2008. Genesis and rank distribution of Upper Carboniferous coal basins in the Cantabrian Mountains, Northern Spain. *International Journal of Coal Geology* 76, 187–204.

Corrales, I., 1971. La sedimentación durante el Estefaniense B–C en Cangas de Narcea, Rengos y Villablino (NW de España). *Trabajos de Geología* 3, 69–75.

Colmenero, J.R., Águeda, J.A., Bahamonde, J.R., Barba, F.J., Barba, P., Fernández, C.I., Salvador, C.I., 1993. Evolución de la Cuenca de Antepais Namuriense y Westfaliense de la Zona Cantábrica. NO. de España. C.R. XII ICC-P, vol. 2. Buenos Aires, pp. 175–190.

Colmenero, J.R., Fernández, L.P., Moreno, C., Bahamonde, J.R., Barba, P., Heredia, N., González, F., 2002. Carboniferous. In: Gibbons, W., Moreno, M.T. (Eds.), *The Geology of Spain*. Geological Society, London, pp. 93–116.

D'Lemos, R.S., Strachan, R.A., Topley, C.G., 1990. The Cadomian orogeny in the North Armorican Massif: a brief review. *Geological Society of London, Special Publication* 51.

Dallmeyer, R.D., Martínez Catalán, J.R., Arenas, R., Gil Ibarguchi, J.I., Gutiérrez-Alonso, G., Fariás, P., Bastida, F., Aller, J., 1997. Diachronous Variscan tectonothermal activity in the NW Iberian Massif: evidence from ⁴⁰Ar/³⁹Ar dating of regional fabrics. *Tectonophysics* 277, 307–337.

DePaolo, D.J., 1981. Neodymium isotopes in the Colorado front range and crust–mantle evolution in the Proterozoic. *Nature* 291, 193–196.

DePaolo, D.J., 1988. *Neodymium Isotope Geochemistry: An Introduction*. Springer Verlag, New York.

DePaolo, D.J., Wasserburg, G.J., 1976. Nd isotopic variations and petrogenetic models. *Geophysical Research Letters* 3, 249–252.

Díez Fernández, R., Catalán, J.R.M., Gerdes, A., Abati, J., Arenas, R., Fernández-Suárez, J., 2010. U–Pb ages of detrital zircons from the Basal allochthonous units of NW Iberia:

- provenance and paleoposition on the northern margin of Gondwana during the Neoproterozoic and Paleozoic. *Gondwana Research* 18, 385–399.
- Díez Fernández, R., Castiñeira, P., Gómez Barreiro, J., 2012. Age constraints on Lower Paleozoic convection system: magmatic events in the NW Iberian Gondwana margin. *Gondwana Research* 21, 1066–1079.
- Díez Montes, A., 2006. La Geología del Dominio “Ollo de Sapo” en las comarcas de Sanabria y Terra do Bolo. (PhD Thesis) Universidad de Salamanca (496 pp.).
- Dostal, J., Keppie, J.D., 2009. Geochemistry of low-grade clastic rocks in the Acatlán Complex of southern Mexico: evidence for local provenance in felsic-intermediate igneous rocks. *Sedimentary Geology* 222, 241–253.
- Dostal, J., Dupuy, C., Caby, R., 1994. Geochemistry of the Neoproterozoic Tilemsi belt of Iforas (Mali, Sahara): a crustal section of an oceanic island arc. *Precambrian Research* 65, 55–69.
- Fernández-Suárez, J., Gutiérrez-Alonso, G., Jenner, G.A., Jackson, S.E., 1998. Geochronology and geochemistry of the Pola de Allande granitoids. Their bearing on the Cadomian/ Avalonian evolution of NW Iberia. 1998. *Canadian Journal of Earth Sciences* 35, 1439–1453.
- Fernandez-Suarez, J., Gutierrez-Alonso, G., Jenner, G.A., Tubrett, M.N., 1999. Crustal sources in Lower Paleozoic rocks from NW Iberia: insights from laser ablation U–Pb ages of detrital zircons. *Journal of the Geological Society* 156, 1065–1068.
- Fernandez-Suarez, J., Gutierrez-Alonso, G., Jenner, G.A., Tubrett, M.N., 2000. New ideas on the Proterozoic–Early Paleozoic evolution of NW Iberia: insights from U–Pb detrital zircon ages. *Precambrian Research* 102, 185–206.
- Fernández-Suárez, J., Alonso, G.G., Cox, R., Jenner, G.A., 2002. Assembly of the Armorica microplate: a strike-slip terrane delivery? Evidence from U–Pb ages of detrital zircons. *Journal of Geology* 110, 619–626.
- Fernandez-Suarez, J., Arenas, R., Jeffries, T.E., Whitehouse, M.J., Villaseca, C., 2006. A U–Pb study of zircons from a lower crustal granulite xenolith of the Spanish central system: a record of Iberian lithospheric evolution from the Neoproterozoic to the Triassic. *Journal of Geology* 114, 471–483.
- Fernández-Suárez, J., Gutierrez-Alonso, G., Johnston, S.T., Jeffries, T.E., Pastor-Galán, D., Jenner, G.A., Murphy, J.B., 2011. Iberian late-Variscan granitoids: some considerations on crustal sources and the significance of “mantle extraction ages”. *Lithos* 123, 121–132.
- Fernández-Suárez, J., Gutiérrez-Alonso, G., Pastor-Galán, D., Hofmann, M., Murphy, J.B., Linnemann, U., 2013. The Ediacaran–Early Cambrian detrital zircon record of NW Iberia: possible sources and paleogeographic constraints. *International Journal of Earth Sciences*. <http://dx.doi.org/10.1007/s00531-013-0923-3> (in press).
- Ferretti, A., Cavalazzi, B., Barbieri, R., Westall, F., Foucher, F., Todesco, R., 2012. From black-and-white to colour in the Silurian. *Palaeogeography, Palaeoclimatology, Palaeoecology* 367–368, 178–192.
- Fuenlabrada, J.M., Arenas, R., Díez Fernández, R., Sánchez Martínez, S., Abati, J., López Carmona, A., 2012. Sm–Nd isotope geochemistry and tectonic setting of the metasedimentary rocks from the basal allochthonous units of NW Iberia (Variscan suture, Galicia). *Lithos* 148, 196–208.
- Frings, K.H., Warr, L.N., 2012. Hydrothermally altered mudrock of the Cñera-Matallana coal basin, Cantabrian Zone, northern Spain. *European Journal of Mineralogy* 24, 1017–1029.
- García Ramos, J.C., Colmenero, J.R., 1981. Evolución sedimentaria y paleogeográfica durante el Devónico en la Cordillera Cantábrica. *Real Academia de Ciencias Exactas, Físicas y Naturales* 2, 61–76.
- García-López, S., Brime, C., Valín, M.L., Sanz-López, J., Bastida, F., Aller, J., Blanco-Ferrera, S., 2007. Tectonothermal evolution of a foreland fold and thrust belt: the Cantabrian Zone (Iberian Variscan belt, NW Spain). *Terra Nova* 19, 469–475.
- García-Ramos, J.C., 1978. Estudio e interpretación de las principales facies sedimentarias comprendidas en las formaciones Naranco y Huergas (Devónico Medio) de la Cordillera Cantábrica (Asturias y León). *Trabajos de Geología* 10, 195–240.
- Gasparrini, M., Bakker, R.J., Bechstadt, T., Boni, M., 2003. Hot dolomites in a Variscan foreland belt: hydrothermal flow in the Cantabrian Zone (NW Spain). *Journal of Geochemical Exploration* 78–9, 501–507.
- Gasparrini, M., Bakker, R.J., Bechstadt, T., 2006. Characterization of dolomitizing fluids in the Carboniferous of the Cantabrian Zone (NW Spain): a fluid-inclusion study with cryo-Raman spectroscopy. *Journal of Sedimentary Research* 76, 1304–1322.
- Gibbons, W., Moreno, T.D. (Eds.), 2002. *The Geology of Spain*. Geological Society of London, London (649 pp.).
- Gloaguen, E., Branquet, Y., Boulvais, P., Moëlo, Y., Chauvel, J.-J., Chiappero, P.-J., Marcoux, E., 2007. Paleozoic oolitic ironstone of the French Armorican Massif: a chemical and structural trap for orogenic base metal–As–Sb–Au mineralisation during Hercynian strike-slip deformation. *Mineralium Deposita* 42, 399–422.
- Guerrak, S., 1987a. Metallogenesis of cratonic oolitic ironstone deposits in the Bled el Mass, Azzel Ma Catalán tti, Ahnet and Mouydir basins, Central Sahara, Algeria. *Geologische Rundschau* 76, 903–922.
- Guerrak, S., 1987b. Paleozoic oolitic ironstones of the Algerian Sahara: a review. *Journal of African Earth Sciences* 6, 1–8.
- Gutiérrez-Alonso, G., 1996. Strain partitioning in the footwall of the Somiedo Nappe: structural evolution of the Narcea Tectonic window, NW Spain. *Journal of Structural Geology* 18, 1217–1229.
- Gutiérrez-Alonso, G., Nieto, F., 1996. White-mica “crystallinity”, finite strain and cleavage development across a large Variscan structure, NW Spain. *Journal of the Geological Society* 153, 287–299.
- Gutierrez-Alonso, G., Fernandez-Suarez, J., Jeffries, T.E., Jenner, G.A., Tubrett, M.N., Cox, R., Jackson, S.E., 2003. Terrane accretion and dispersal in the northern Gondwana margin. An Early Paleozoic analogue of a long-lived active margin. *Tectonophysics* 365, 221–232.
- Gutiérrez-Alonso, G., Fernández-Suárez, J., Weil, A.B., 2004. Orocline triggered lithospheric delamination. Orogenic Curvature: Integrating Paleomagnetic and Structural Analyses. In: Sussman, A.J., Weil, A.B. (Eds.), *Geological Society of America Special Paper*, vol. 383, pp. 121–130.
- Gutiérrez-Alonso, G., Fernández-Suárez, J., Collins, Alan S., Abad, I., Nieto, F., 2005. Amazonian Mesoproterozoic basement in the core of the Ibero-Armorican Arc: $^{40}\text{Ar}/^{39}\text{Ar}$ detrital mica ages complement the zircon's tale. *Geology* 33, 637–640.
- Gutiérrez-Alonso, G., Fernández-Suárez, J., Gutiérrez-Marco, J.C., Corfu, F., Murphy, J.B., Suárez, M., 2007. U–Pb depositional age for the upper Barrios Formation (Armorican Quartzite facies) in the Cantabrian zone of Iberia: implications for stratigraphic correlation and paleogeography. The Evolution of the Rheic Ocean: From Avalonian–Cadomian Active Margin to Alleghenian–Variscan Collision. In: Linnemann, U., Nance, R.D., Kraft, P., Zulauf, G. (Eds.), *Geological Society of America Special Paper*, vol. 423, pp. 287–296.
- Gutiérrez-Alonso, G., Fernández-Suárez, J., Weil, A.B., Murphy, J.B., Nance, R.D., Corfu, F., Johnston, S.T., 2008. Self-subduction of the Pangean global plate. *Nature Geoscience* 1, 549–553.
- Gutiérrez-Alonso, G., Fernández-Suárez, J., Jeffries, T., Collins, A.S., Johnston, S.T., González-Clavijo, E., Pastor-Galán, D., 2010. Delimitação mediante idades absolutas ($^{40}\text{Ar}/^{39}\text{Ar}$ e U–Pb) do desenvolvimento oroclinal e da delaminação litosférica associada no Arco Ibero Armoricano. *Revista Electrónica de Ciências da Terra* 23–24. Gutiérrez-Alonso, G., Murphy, J.B., Fernández-Suárez, J., Weil, A.B., Franco, M.P., Gonzalo, J.C., 2011a. Lithospheric delamination in the core of Pangea: Sm–Nd insights from the Iberian mantle. *Geology* 39, 155–159.
- Gutiérrez-Alonso, G., Fernández-Suárez, J., Jeffries, T.E., Johnston, S.T., Pastor-Galán, D., Murphy, J.B., Franco, M.P., Gonzalo, J.C., 2011b. Diachronous post-orogenic magmatism within a developing orocline in Iberia, European Variscides. *Tectonics* 30, 17.
- Gutiérrez-Alonso, G., Johnston, S.T., Weil, A.B., Pastor-Galán, D., Fernández-Suárez, J., 2012. Buckling an orogen: the Cantabrian Orocline. *GSA Today* 22, 4–9.
- Gutiérrez-Marco, J.C., Aramburu, C., Arbizu, M., Bernárdez, E., Hacar Rodríguez, M.P., Méndez-Bedia, I., Montesinos López, R., Rábano, I., Truyols, J., Villas, E., 1999. Revisión bioestratigráfica de las pizarras del Ordovícico Medio en el noroeste de España (zonas Cantábrica, Asturoccidental-leonesa y Centroibérica septentrional). *Acta Geologica Hispánica* 34, 3–87.
- Gutiérrez-Marco, J.C., Robardet, M., Rábano, I., Sarmiento, G.N., San José Lancha, M.A., Herranz, P., Pieren Pidal, A.P., 2002. Ordovician. In: Gibbons, W., Moreno, Y. (Eds.), *The Geology of Spain*, Geological Society (London), pp. 31–49.
- Heinz, W., Loeschke, J., Vavra, G., 1985. Phreatomagmatic volcanism during the Ordovician of the Cantabrian Mountains. *Geologische Rundschau* 74, 623–639.
- Hofmann, M.H., Keller, M., 2006. Sequence stratigraphy and carbonate platform organization of the Devonian Santa Lucia Formation, Cantabrian Mountains, NW-Spain. *Facies* 52, 149–157.
- Julivert, M., Arborely, M.L., 1986. Areal balancing and estimate of areal reduction in a thin-skinned fold-and-thrust belt (Cantabrian Zone, NW Spain) — constraints on its emplacement mechanism. *Journal of Structural Geology* 8, 407–414.
- Julivert, M., Marcos, A., 1973. Superimposed folding under flexural conditions in the Cantabrian Zone (Hercynian Cordillera, northwest Spain). *American Journal of Science* 273, 353–375.
- Keller, M., Bahlburg, H., Reuther, C.D., 2008. The transition from passive to active margin sedimentation in the Cantabrian Mountains, Northern Spain: Devonian or Carboniferous? *Tectonophysics* 461, 414–427.
- Kerr, A., Jenner, G.A., Fryer, B.J., 1995. Sm–Nd isotopic geochemistry of Precambrian to Paleozoic granulite suites and the deep-crustal structure of the southeast margin of the Newfoundland Appalachians. *Canadian Journal of Earth Sciences* 32, 224–245.
- Kubler, B., 1968. Evaluation quantitative du métamorphisme par la cristallinité de l'illite. *Bull. Centres Rech. Pau-SNPA* 2, 385–397.
- Li, Q., Liu, S., Han, B., Zhang, J., Chu, Z., 2005. Geochemistry of metasedimentary rocks of the Proterozoic Xingxingxia complex: implications for provenance and tectonic setting of the eastern segment of the Central Tianshan Tectonic Zone, northwestern China. *Canadian Journal of Earth Sciences* 42, 287–306.
- Linnemann, U., McNaughton, N.J., Romer, R.L., Gehmlich, M., Drost, K., Tonk, C., 2004. West African provenance for Saxo-Thuringia (Bohemian Massif): did Armorica ever leave pre-Pangean Gondwana? U/Pb-SHRIMP zircon evidence and the Nd-isotopic record. *International Journal of Earth Sciences* 93, 683–705.
- Linnemann, U., Gerdes, A., Drost, K., Buschmann, B., 2007. The continuum between Cadomian orogenesis and opening of the Rheic Ocean: constraints from LA-ICP-MS U–Pb zircon dating and analysis of plate-tectonic setting (Saxo-Thuringian zone, northeastern Bohemian Massif, Germany). *Geological Society of America Special Papers* 423, 61–96.
- Linnemann, U., Pereira, F., Jeffries, T.E., Drost, K., Gerdes, A., 2008. The Cadomian Orogeny and the opening of the Rheic Ocean: the diachrony of geotectonic processes constrained by LA-ICP-MS U–Pb zircon dating (Ossa-Morena and Saxo-Thuringian Zones, Iberian and Bohemian Massifs). *Tectonophysics* 461, 21–43.
- Loneragan, L., Johnson, C., 1998. Reconstructing orogenic exhumation histories using synorogenic detrital zircons and apatites: an example from the Betic Cordillera, SE Spain. *Basin Research* 10, 353–364.
- Longerich, H.R., Jenner, G.A., Fryer, B.J., Jackson, S.E., 1990. Inductively coupled plasma-mass spectrometric analysis of geological samples: a critical evaluation based on case studies. *Chemical Geology* 83, 105–118.
- López-Guijarro, R., Armendáriz, M., Quesada, Cecilio, Fernández-Suárez, Javier, Brendan Murphy, J., Pin, C., Bellido, Felix, 2008. Ediacaran–Paleozoic tectonic evolution of the Ossa Morena and Central Iberian zones (SW Iberia) as revealed by Sm/Nd isotope systematics. *Tectonophysics* 461, 202–214.
- Lotze, F., 1945. Zur gliederung der Variszischen der Iberischen Meseta. *Geotektonische Forschungen* 6, 78–92.
- Marcos, A., Pulgar, J.A., 1982. An approach to the tectonostratigraphic evolution of the Cantabrian foreland thrust and fold belt, Hercynian Cordillera of NW Spain. *Neues Jahrbuch für Geologie und Paläontologie Abhandlungen* 163 (2), 256–260.
- Martínez Catalán, J.R., 2011. Are the oroclines of the Variscan belt related to late Variscan strike-slip tectonics? *Terra Nova* 23, 241–247.

- Martínez Catalán, J.R., 2012. The Central Iberian arc, an orocline centered in the Iberian Massif and some implications for the Variscan belt. *International Journal of Earth Sciences* 1–16.
- Martínez Catalán, J.R., Arenas, R., Díaz García, F., Gómez-Barreiro, J., González Cuadra, P., Abati, J., Castiñeiras, P., Fernández-Suárez, J., Sánchez Martínez, S., Andonaegui, P., González Clavijo, E., Díez Montes, A., Rubio Pascual, F.J., Valle Aguado, B., 2007. Space and time in the tectonic evolution of the northwestern Iberian Massif: implications for the comprehension of the Variscan belt. In: Hatcher Jr., R.D., Carlson, M.P., McBride, J.H., Martínez Catalán, J.R. (Eds.), 4-D Framework of Continental Crust: Geological Society of America Memoir, 200, pp. 403–423. [http://dx.doi.org/10.1130/2007.1200\(21\)](http://dx.doi.org/10.1130/2007.1200(21)).
- Martínez Catalán, J.R., Arenas, R., Abati, J., Sánchez Martínez, Sonia, Díaz García, Florentino, Fernández Suárez, Javier, González Cuadra, Pablo, Castiñeiras, Pedro, Gómez Barreiro, Juan, Díez Montes, Alejandro, González Clavijo, Emilio, Rubio, Francisco J., Andonaegui Pascual, Pilar, Jeffries, Teresa E., Alcock, James E., Díez Fernández, Rubén, López Carmona, A., 2009. A rootless suture and the loss of the roots of a mountain chain: the Variscan belt of NW Iberia. *Comptes Rendus Geosciences* 341, 114–126.
- Martínez, F.J., Reche, J., Iriando, A., 2008. U–Pb Shrimp-RG zircon ages of Variscan igneous rocks from the Guillerías massif (NE Iberia pre-Mesozoic basement). Geological implications. *Comptes Rendus Geoscience* 340, 223–232.
- Martínez-García, E., 1981. El Paleozoico de la Zona Cantábrica Oriental (Noroeste de España). *Trabajos de Geología* 11, 95–127.
- Martínez-García, E., 1991. Hercynian synorogenic and postorogenic successions in the Cantabrian and Palentian Zobs, NW Spain. Comparisons with other western European occurrences. *Giornale di Geologia* 53, 209–228.
- Martin-Izard, A., Fuertes-Fuente, M., Cepedal, A., Moreiras, D., Nieto, J.G., Maldonado, C., Pevida, L.R., 2000. The Rio Narcea gold belt intrusions: geology, petrology, geochemistry and timing. *Journal of Geochemical Exploration* 71, 103–117.
- McCulloch, M.T., Wasserburg, G.J., 1978. Sm–Nd and Rb–Sr chronology of continental crust formation. *Science* 200, 1003–1011.
- McLaughlin, P.I., Emsbo, P., Brett, C.E., 2012. Beyond black shales: the sedimentary and stable isotope records of oceanic anoxic events in a dominantly oxic basin (Silurian; Apalachian Basin, USA). *Palaeogeography, Palaeoclimatology, Palaeoecology* 367–368, 153–177.
- McLennan, S.M., 2001. Relationships between the trace element composition of sedimentary rocks and upper continental crust. *Geochemistry, Geophysics, Geosystems* 2.
- McLennan, S., Hemming, S., McDaniel, D., Hanson, G., 1993. In: Johnsson, M., Basu, A. (Eds.), *Geochemical Approaches to Sedimentation, Provenance, and Tectonics*. Geological Society of America.
- Meinhold, G., Kostopoulos, D., Reischmann, T., 2007. Geochemical constraints on the provenance and depositional setting of sedimentary rocks from the islands of Chios, Inousses and Psara, Aegean Sea, Greece: implications for the evolution of Palaeotethys. *Journal of the Geological Society* 164–6, 1145–1163.
- Merino-Tomé, O.A., Bahamonde, J.R., Colmenero, J.R., Heredia, N., Villa, E., Farias, P., 2009. Emplacement of the Cuera and Picos de Europa imbricate system at the core of the Iberian-Armorican arc (Cantabrian zone, north Spain): new precisions concerning the timing of arc closure. *Geological Society of America Bulletin* 121, 729–751.
- Montero, P., Bea, F., González-Lodeiro, F., Talavera, C., Whitehouse, M.J., 2007. Zircon ages of metavolcanic rocks and metagranites of the Olla de Sapo Domain in Central Spain: implications of Neoproterozoic to Early Paleozoic evolution of Iberia. *Geological Magazine* 144, 963–976.
- Montero, P., Talavera, C., Bea, F., González-Lodeiro, F., Whitehouse, M.J., 2009. Zircon geochronology and the age of the Cambro-Ordovician rifting in Iberia. *Journal of Geology* 117, 174–191.
- Murphy, J.B., Nance, R.D., 1989. A model for the evolution of the Avalonian–Cadomian belt. *Geology* 17, 735–738.
- Murphy, J.B., Nance, R.D., 2002. Sm–Nd isotopic systematics as tectonic tracers: an example from West Avalonia in the Canadian Appalachians. *Earth-Science Reviews* 59, 77–100.
- Murphy, J.B., Strachan, R.A., Nance, R.D., Parker, K.D., Fowler, M.B., 2000. Prot-Avalonia: A 1.2–1.0 Ga tectonothermal event and constraints for the evolution of Rodinia. *Geology* 28, 1071–1074.
- Murphy, J.B., Gutiérrez-Alonso, G., Nance, R.D., Fernández-Suárez, J., Keppie, J.D., Quesada, C., Strachan, R.A., Dostal, J., 2006. Origin of the Rheic Ocean: rifting along a Neoproterozoic suture? *Geology* 34, 325–328.
- Murphy, J.B., Gutiérrez-Alonso, G., Fernández-Suárez, J., Braid, J.A., 2008. Probing crustal and mantle lithosphere origin through Ordovician volcanic rocks along the Iberian passive margin of Gondwana. *Tectonophysics* 461 (1–4), 166–180.
- Nance, R.D., Linnemann, U., 2008. The Rheic Ocean: origin, evolution, and significance. *GSA Today* 18, 4.
- Nance, R.D., Gutiérrez-Alonso, G., Keppie, J.D., Linnemann, U., Murphy, J.B., Quesada, C., Strachan, R.A., Woodcock, N.H., 2010. Evolution of the Rheic Ocean. *Gondwana Research* 17, 194–222.
- Nie, J., Horton, B.K., Mora, A., Saylor, J.E., Housh, T.B., Rubiano, J., Naranjo, J., 2010. Tracking exhumation of Andean ranges bounding the Middle Magdalena Valley Basin, Colombia. *Geology* 38, 451–454.
- Nieto, F., Sanchez-Navas, A., 1994. A comparative XRD and TEM study of the physical meaning of the white mica «crystallinity» index. *European Journal of Mineralogy* 6, 611–621.
- Pastor-Galán, D., 2013. Evolución geodinámica del orocline Ibero-Armoricano. *Geología estructural, modelización análoga y geocronología*. 183 p. Nova Terra, 43, A Coruña.
- Pastor-Galán, D., Mulchrone, K.F., 2009. Factors affecting finite strain estimation in low-grade, low-strain clastic rocks. *Journal of Structural Geology* 31 (12), 1586–1596.
- Pastor-Galán, D., Gutiérrez-Alonso, G., Weil, A.B., 2011. Orocline timing through joint analysis: insights from the Ibero-Armorican Arc. *Tectonophysics* 507, 31–46.
- Pastor-Galán, D., Gutiérrez-Alonso, G., Weil, A.B., Fernández-Suárez, J., Johnston, S.T., Murphy, J.B., 2012a. A virtual tour of the Ibero-Armorican orocline. *Journal of the Virtual Explorer* 43.
- Pastor-Galán, D., Gutiérrez-Alonso, G., Zuluaga, G., Zanella, F., 2012b. Analogue modeling of lithospheric-scale orocline buckling: constraints on the evolution of the Iberian-Armorican Arc. *Geological Society of America Bulletin* 124, 1293–1309.
- Pastor-Galán, D., Gutiérrez-Alonso, G., Mulchrone, K.F., Huerta, P., 2012c. Conical folding in the core of an orocline. A geometric analysis from the Cantabrian Arc (Variscan Belt of NW Iberia). *Journal of Structural Geology* 39, 210–223.
- Pastor-Galán, D., Gutiérrez-Alonso, G., Dietl, C., Zanella, F., 2012d. Modelización análoga del desprendimiento de una raíz litosférica. ¿Puede un orocline producir el desprendimiento del manto litosférico? *Geogaceta* 52, 123–126.
- Pastor-Galán, D., Gutiérrez-Alonso, G., Murphy, J.B., Fernández-Suárez, J., Hofmann, M., Linnemann, U., 2013. Provenance analysis of the Paleozoic sequences of the northern Gondwana margin in NW Iberia: passive margin to Variscan collision and orocline development. *Gondwana Research* 23, 1089–1103.
- Pereira, M.F., Linnemann, U., Hofmann, M., Chichorro, M., Solá, A.R., Medina, J., Silva, J.B., 2012. The provenance of Late Ediacaran and Early Ordovician siliciclastic rocks in the Southwest Central Iberian Zone: constraints from detrital zircon data on northern Gondwana margin evolution during the late Neoproterozoic. *Precambrian Research* 192–195, 166–189.
- Pérez-Estaún, A., Bastida, F., Alonso, J.L., Marquinez, J., Aller, J., Alvarezmarrón, J., Marcos, A., Pulgar, J.A., 1988. A thin-skinned tectonics model for an arcuate fold and thrust belt — the Cantabrian Zone (VARISCAN Ibero-Armorican Arc). *Tectonics* 7, 517–537.
- Pérez-Estaún, A., Pulgar, J.A., Banda, E., Alvarez-Marrón, J., ESCI-N Research Group, 1994. Crustal structure of the external Variscides in NW Spain from deep seismic reflection profiling. *Tectonophysics* 232, 91–118.
- Quesada, C., 1991. Geological constraints on the Paleozoic tectonic evolution of tectonostratigraphic terranes in the Iberian Massif. *Tectonophysics* 185, 225–245.
- Quesada, C., 2006. The Ossa-Morena Zone of the Iberian Massif: a tectonostratigraphic approach to its evolution. *Zeitschrift der Deutschen Gesellschaft für Geowissenschaften* 157, 585–595.
- Robardet, M., 2002. Alternative approach to the Variscan Belt in southwestern Europe: preorogenic paleobiogeographical constraints. In: Martínez Catalán, J.R., Hatcher, R.D., Arenas, R., Díaz García, F. (Eds.), *Variscan–Appalachian Dynamics: The Building of the Late Paleozoic Basement*. Geological Society of America Special Paper, 364, pp. 1–15.
- Robardet, M., 2003. The Armorica ‘microplate’: fact or fiction? Critical review of the concept and contradictory paleobiogeographical data. *Palaeogeography, Palaeoclimatology, Palaeoecology* 195, 125–148 (24).
- Rodríguez-Fernández, L.R., 1991. Evolución tectonosedimentaria del NO del Macizo Ibérico durante el Carbonífero. *Cuaderno Lab. Xeológico de Laxe* 16, 37–52.
- Roser, B.P., Korsch, R.J., 1986. Determination of tectonic setting of sandstone– mudstone suites using $\text{SiO}_2/\text{K}_2\text{O}$ and $\text{K}_2\text{O}/\text{Na}_2\text{O}$ ratio. *Journal of Geology* 94, 635–650.
- Rubio Ordóñez, Á., 2010. Magmatismo Neoproterozoico en el Antiforme del Narcea. PhD thesis, Universidad de Oviedo. 306 pp. Unpublished.
- Rubio-Ordóñez, Á., Valverde-Vaquero, P., Corretgé, L.G., Cuesta-Fernández, A., Gallastegui, G., Fernández-González, M., Gerdes, A., 2012. An Early Ordovician tonalitic–granodioritic belt along the Schistose–Greywacke Domain of the Central Iberian Zone (Iberian Massif, Variscan Belt). *Geological Magazine* 149, 927–939.
- Rubio-Ordóñez, Á., Gutiérrez-Alonso, G., Valverde-Vaquero, P., Cuesta, A., Gallastegui, G., Gerdes, A., Cárdenas, V., 2013. Arc-related Ediacaran magmatism along the northern margin of Gondwana: geochronology and isotopic geochemistry from northern Iberia. *Gondwana Research* (in press).
- Ryan, K.M., Williams, D.M., 2007. Testing the reliability of discrimination diagrams for determining the tectonic depositional environment of ancient sedimentary basins. *Chemical Geology* 242, 103–125.
- Sánchez-García, T., Bellido, F., Quesada, C., 2003. Geodynamic setting and geochemical signatures of Cambrian–Ordovician rift-related igneous rocks (Ossa-Morena Zone, SW Iberia). *Tectonophysics* vol. 365 (1–4), 233–255 (24 April).
- Sanchez-Garcia, T., Quesada, C., Bellido, F., Dunning, G.R., Del Tanago, J.G., 2008. Two-step magma flooding of the upper crust during rifting: the Early Paleozoic of the Ossa Morena Zone (SW Iberia). *Tectonophysics* 461, 72–90.
- Shaw, J., Johnston, S.T., Gutiérrez-Alonso, G., Weil, A.B., 2012. Oroclines of the Variscan orogen of Iberia: paleocurrent analysis and paleogeographic implications. *Earth and Planetary Science Letters* 329–330, 60–70.
- Shaw, J., Gutiérrez-Alonso, G., Johnston, S.T., Pastor Galán, D., Hofmann, M., 2013. Provenance variability along the Lower Ordovician north Gondwana margin: Paleogeographic and tectonic implications of U–Pb detrital zircon ages from the Armorican Quartzite of the Iberian Variscan belt (in press).
- Spalletti, L.A., Limarino, C.O., Piñol, F.C., 2012. Petrology and geochemistry of Carboniferous siliciclastics from the Argentine Frontal Cordillera: a test of methods for interpreting provenance and tectonic setting. *Journal of South American Earth Sciences* 36, 32–54.
- Stampfli, G.M., Borel, G.D., 2002. A plate tectonic model for the Paleozoic and Mesozoic constrained by dynamic plate boundaries and restored synthetic oceanic isochrons. *Earth and Planetary Science Letters* 196, 17–33.
- Stampfli, G.M., Hochard, C., Vérard, C., Wilhem, C., von Raumer, J., 2013. The formation of Pangea. *Tectonophysics* 593, 1–19.
- Steiger, R.H., Jager, E., 1978. Subcommission on geochronology: convention on the use of decay constants in geochronology and cosmochronology. 116, 67–71.
- Stewart, R.J., Hallet, B., Zeitler, P.K., Malloy, M.A., Allen, C.M., Trippett, D., 2008. Brahmaputra sediment flux dominated by highly localized rapid erosion from the easternmost Himalaya. *Geology* 36, 711–714.

- García-López, S., Bastida, F., Aller, J., Sanz-López, J., Marín, J.A., Blanco-Ferrera, S., 2013. Tectonothermal evolution of a major thrust system: the Esla-Valsurbio unit (Cantabrian Zone, NW Spain). *Geological Magazine* 150 (6), 1047–1061 (November). Cambridge University Press.
- Suárez, A., 1988. Estructura del área de Villaviciosa-Libardón (Asturias, Cordillera Cantábrica). *Trabajos de Geología* 17, 87–98.
- Suárez de Centi, C., 1988. Estratigrafía, sedimentología y paleogeografía de la Formación Furada/San Pedro. Zona Cantábrica (NW de España). (PhD Thesis) Universidad de Oviedo (530 pp.).
- Tait, J., 1999. New Early Devonian paleomagnetic data from NW France: paleogeography and implications for the Armorican microplate hypothesis. *Journal of Geophysical Research* 104, 2831–2839.
- Tait, J., Bachtadse, V., Soffel, H., 1994. New palaeomagnetic constraints on the position of central Bohemia during Early Ordovician times. *Geophysical Journal International* 116, 131–140.
- Taylor, S.R., McLennan, S.M., 1985. *The Continental Crust: Its Composition and Evolution*. Blackwell Scientific Pub., Palo Alto, CA.
- Taylor, K.G., Simo, J.A. (Toni), Yocum, D., Leckie, D.A., 2002. Stratigraphic significance of ooidal ironstones from the Cretaceous Western Interior Seaway: the Peace River Formation, Alberta, Canada, and the Castlegate Sandstone, Utah, U.S.A. *Journal of Sedimentary Research* 72, 316–327.
- Torsvik, T.H., Cocks, L.R.M., 2004. Earth geography from 400 to 250 Ma: a palaeomagnetic, faunal and facies review. *Journal of the Geological Society* 161, 555–572.
- Torsvik, T.H., Van der Voo, R., Preenen, U., Mac Niocaill, C., Steinberger, B., Doubrovine, P.V., van Hinsbergen, D.J.J., Domeier, M., Gaina, C., Tohver, E., Meert, J.G., McCausland, P.J.A., Cocks, L.R.M., 2012. Phanerozoic polar wander, palaeogeography and dynamics. *Earth Science Reviews* 114, 325–368.
- Ugidos, J.M., Armenteros, I., Barba, P., Valladares, M.I., Colmenero, J.R., 1997. Geochemistry and petrology of recycled orogen-derived sediments: a case study from Upper Pre-Cambrian siliciclastic rocks of the Central Iberian Zone, Iberian Massif, Spain. *Precambrian Research* 84, 163–180.
- Ugidos, J.M., Billstrom, K., Valladares, M.I., Barba, P., 2003. Geochemistry of the upper neoproterozoic and lower Cambrian siliciclastic rocks and U–Pb dating on detrital zircons in the Central Iberian Zone, Spain. *International Journal of Earth Sciences* 92, 661–676.
- Valladares, M.I., Ugidos, J.M., Barba, P., Colmenero, J.R., 2002. Contrasting geochemical features of the Central Iberian Zone shales (Iberian Massif, Spain): implications for the evolution of Neoproterozoic–Lower Cambrian sediments and their sources in other peri-Gondwanan areas. *Tectonophysics* 352, 121–132.
- Valverde-Vaquero, P., Dunning, G.R., 2000. New UPb ages for Early Ordovician magmatism in central Spain. *Journal of the Geological Society* 157, 15–26.
- Valverde-Vaquero, P., Marcos, A., Farias, P., Gallastegui, G., 2006. U–Pb dating of Ordovician felsic volcanism in the schistose domain of the Galicia-Trás-os-Montes zone near Cabo Ortegal (NW Spain). *Geologica Acta* 3, 27–37.
- Van Der Voo, R., 1982. Pre-Mesozoic paleomagnetism and plate tectonics. *Annual Review of Earth and Planetary Sciences* 10, 191–220.
- Van Der Voo, R., 1988. Paleozoic paleogeography of North America, Gondwana, and intervening displaced terranes: comparisons of paleomagnetism with paleoclimatology and biogeographical patterns. *Geological Society of America Bulletin* 100, 311–324.
- Van der Voo, R., 1993. *Paleomagnetism of the Atlantic, Tethys and Iapetus Oceans*. ix + 411 pp. Cambridge University Press, Cambridge, New York, Port Chester, Melbourne, Sydney.
- Van Houten, F.B., 1985. Oolitic ironstones and contrasting Ordovician and Jurassic paleogeography. *Geology* 13, 722–724.
- Van Houten, Franklyn B., 1990. Palaeozoic oolitic ironstones on the North American craton. *Palaeogeography, Palaeoclimatology, Palaeoecology* 80, 245–254.
- Van Houten, F.B., Arthur, M.A., 1989. Temporal patterns among Phanerozoic oolitic ironstones and oceanic anoxia. *Geological Society of London, Special Publication* 46, 33–49.
- Weil, A.B., 2006. Kinematics of oroclinal tightening in the core of an arc: paleomagnetic analysis of the Ponga Unit, Cantabrian Arc, northern Spain. *Tectonics* 25, 1–23.
- Weil, A.B., Van der Voo, R., Van der Pluijm, B.A., 2001. Oroclinal bending and evidence against the Pangea megashear: the Cantabria–Asturias arc (northern Spain). *Geology* 29, 991–994.
- Weil, A.B., Gutiérrez-Alonso, G., Conan, J., 2010. New time constraints on lithospheric-scale oroclinal bending of the Ibero-Armorican arc: A palaeomagnetic study of earliest Permian rocks from Iberia. *Journal of the Geological Society of London* 167, 127–143.
- Weil, A., Brandon, Gutiérrez-Alonso, G., Johnston, S.T., Pastor-Galán, D., 2013. Kinematic constraints on buckling a lithospheric-scale oroclinal along the northern margin of Gondwana: a geologic synthesis. *Tectonophysics* 582, 25–49.
- Weislogel, A.L., Graham, S.A., Chang, E.Z., Wooden, J.L., Gehrels, G.E., 2010. Detrital zircon provenance from three turbidite depocenters of the Middle–Upper Triassic Songpan–Ganzi complex, central China: record of collisional tectonics, erosional exhumation, and sediment production. *Geological Society of America Bulletin* 122, 2041–2062.
- Young, T.P., 1989. Phanerozoic ironstones: an introduction and review. *Geological Society of London, Special Publication* 46, ix–xxv.